

UNIVERSITY OF ILLINOIS

April 17 19 89

THIS IS TO CERTIFY THAT THE THESIS PREPARED UNDER MY SUPERVISION BY

Amy Elizabeth Marks

ENTITLED The Effect of Long-term Potentiation Induction in Vivo

on the Laminar Distribution of Astrocytic Processes in the Hippocampal
Formation

IS APPROVED BY ME AS FULFILLING THIS PART OF THE REQUIREMENTS FOR THE

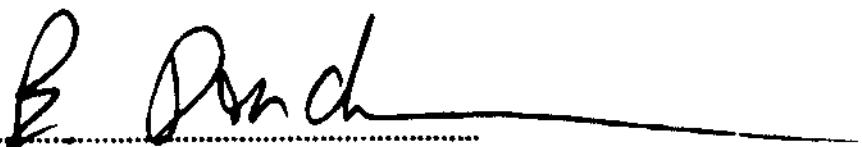
DEGREE OF Bachelor of Science in Psychology

William T. Greenough



Instructor in Charge

APPROVED:



HEAD OF DEPARTMENT OF Psychology

**The Effect of Long-term Potentiation Induction In Vivo
on
the Laminar Distribution of Astrocytic Processes
in the
Hippocampal Formation**

By

Amy Elizabeth Marks

Thesis

**for the
Degree of Bachelor of Science
in
Psychology**

**College of Liberal Arts and Sciences
University of Illinois
Urbana, Illinois**

1989

Table of Contents

| | |
|---|--------------|
| I. Abstract | 1 |
| II. Introduction | 2-17 |
| A. Environmental Complexity Paradigm | 3-6 |
| B. Long-term Potentiation | 6-10 |
| C. GIIa | 10-17 |
| III. Methods | 18-23 |
| A. Part 1 | 18-20 |
| B. Part 2 | 20-23 |
| IV. Results | 23-27 |
| A. Part 1 | 23-24 |
| B. Part 2 | 24-27 |
| V. Discussion | 27-36 |
| VI. Bibliography | 37-42 |
| VII. Author Notes | 43 |
| VIII. Figure Captions | 44-46 |

Abstract

The questions investigated in this experiment are whether or not there exists a laminar pattern of astrocytic process surface density (Sv) and thickness in the rat hippocampal formation, and is this pattern altered by in vivo induction of long-term potentiation (LTP). The distribution and size of astrocytic processes is different for all thirds of the dentate gyrus molecular layer in rats receiving no experimental treatment, with thickness and Sv decreasing as one moves from the outer to the innermost third of the molecular layer. Following potentiating stimulation, there are increases in Sv and thickness of astrocytic processes at 400 μ m from the electrode track in the LTP group that are not found in the activity control group and that are not induced by electrode penetration. Glial processes may increase in size and number in order to more efficiently regulate the changing ionic and osmotic microenvironment that may accompany synaptic potentiation.

Surface Density and Thickness of Hippocampal Astrocytes

The brain has both a great precision of organization and the capacity to process and store information in an organized and consistent fashion, but a causal relationship between alterations in brain structures and information processing remains elusive. Almost 55 years ago Charles Sherrington stated that, "Mental experiences on the one hand, and brain happenings on the other, though I cannot correlate together, I nevertheless find to coincide in time and space." (Sherrington, 1933, p.67).

What are the specific alterations underlying the process of mammalian memory storage? The basic functional wiring of the brain is laid down early in development, but this circuitry can be modified throughout the life of the organism. Both external and internal factors can initiate change in the circuitry of the developing, mature, and aged nervous system, yet the specific elements that demonstrate plasticity are difficult to pinpoint in a causal relationship with a particular factor. Somehow, neurons and glia, as well as other constituents of the vertebrate central nervous system, are organized in a vast and little understood milieu which endows the organism with the ability to adapt to an ever-changing environment.

Approximately 40 years ago it began to become apparent that the brain can be organized by external environmental events. Hebb (1949) found that laboratory rats enriched by the various stimulations of his home environment were better able to negotiate the Hebb-Williams maze in comparison to laboratory rats raised in a nonstimulating and isolated environment. By controlling the organization of events in the external world, investigators could control the organization of information entering the brain. To investigate experienced-induced neuronal changes, the investigator must alter the amount or type of information entering the nervous system, and compare organisms receiving different experimental input. Essentially, there are two main

ways that neuronal connectivity could change in response to information processing. One way of encoding new information would be a qualitative change as evidenced by increased efficacy and processing capacity of existing neuronal elements. A second way of processing information would be the formation of new neuronal elements. In actuality, the changes involved are most likely both qualitative and quantitative, and possibly not exclusively neuronal.

Despite the unquestioned involvement of neurons in learning and memory, they do not exist alone in the microenvironment of the central nervous system. The surrounding neuropil is full of glial cells and blood vessels which undoubtedly can play a role in information processing. The glial cells exist in great numbers within the neuropil, outnumbering neurons by a factor of 10. In the past, glial cells have been viewed as merely the "housekeepers" of the nervous system, performing chores such as scavenging neuronal debris to keep the neuronal environment in optimal functional order. When Rudolph Virchow first described and named the glial cells in 1846, he stated, "Hitherto, considering the nervous system, I have only spoken of the really nervous parts of it. But...it is important to have a knowledge of that substance also which lies between the proper nervous parts, holds them together, and gives the whole its form." (Virchow, 1859, as cited in Kuffler & Nicholls, 1976). In recent years, however, glial cells have been recognized as potentially having a role in the changes that underlie information storage.

Environmental Complexity Paradigm

Following Hebb's observation that laboratory rats raised in a stimulating environment could perform better on maze learning than rats reared with minimal laboratory stimulation, investigators standardized the EC/SC/IC paradigm for studying changes in synaptic components in animals receiving varying degrees of environmental stimulation. In this paradigm, littermate rats are assigned to one of three

environmental conditions. The environmental complexity (EC) condition involves housing 8-14 rats together in a large wire cage filled with play objects of various shapes, colors, and textures which are changed and rearranged daily to provide new environmental configurations for exploration. The individual cage (IC) rats are housed individually in standard laboratory cages with no toys. The social cage (SC) consists of two animals housed together in a cage similar to the IC cage. Rosenzweig and Bennett (1972) showed that rats raised in the EC cage had smaller body weights and heavier total brain weights than SC and IC rats. In 1973, Greenough and Volkmar showed that EC rats had a 20% average increase in dendritic length over the IC's in the pyramidal cells of layers II, IV, and V of the occipital cortex, in comparison to the SC and IC rats. The increased dendritic length may have been related to the increased amount of visual information converging on the occipital cortex of the EC rats. Juraska, Fitch, Henderson, and Rivers (1985) subsequently demonstrated that the increase in dendritic length following exposure to a complex environment is not solely a cortical phenomenon. They reported that female rats raised in an EC environment had more dendrite per neuron in the hippocampal dentate gyrus than females raised in the isolated environment. This difference in dendritic material was not evident in the male rats placed in the same environment.

These results raised questions concerning whether or not the brain maintained plasticity throughout life, or if the ability to change at the level of the neuron was solely a feature of the developing brain. Green, Greenough and Schlumpf (1983) placed adult female rats into either the EC or the IC environment and found that the EC rats had significantly more dendritic material than the IC rats in terms of greater second and fifth order branching, as well as longer terminating branches. From this evidence, it appears that adult rats can maintain brain plasticity, and thus it is likely that plasticity of brain structures is not limited to the developing organism.

The next question that needed to be investigated was whether or not the increased dendritic branching found in the EC rats represented an increase in the number of synapses made by each neuron. Turner and Greenough (1985) used electron microscopy to calculate the number of synapses per neuron in layers I-IV in the occipital cortex of littermate rats raised in EC, SC, or IC conditions. They found that EC rats had the highest synapse per neuron ratio, and IC rats had the lowest. These EC/SC/IC experiments provide evidence that altered synaptic connectivity, and possibly synaptogenesis, are plastic neuronal changes involved in the processing and storage of new information.

While the observed changes in brain structures are believed to be a result of the processing and storage of information, it may also be that the dendritic and synaptic changes occur as a result of a more general bodily phenomenon such as physical exercise, hormonal influences, or metabolic effects. Chang and Greenough (1982) examined the effects of training rats to negotiate a maze while wearing an opaque contact occluder in one of their eyes. To ensure that the visual input associated with maze training was projected to a single hemisphere, the corpus callosum was severed prior to training. They discovered that in unilaterally-occluded trained rats, only the occipital cortex layer V pyramidal neurons contralateral to the nonoccluded eye had increased dendritic length. Furthermore, rats trained with alternating eye occlusion had greater dendritic lengths when compared to control rats that had not been maze trained at all. These results strongly support the proposition that the dendritic changes are due specifically to the processing of visual information rather than a nonspecific training influence.

In summary, the most plausible hypothesis regarding altered patterns of dendritic connectivity following sensory enhancement and deprivation is that these neuronal

changes are the morphological evidence of a new circuitry forming to encode the information associated with novel experience.

Long-term Potentiation

It is difficult to study brain changes that occur in response to learning; one does not know exactly where to look for these changes, and one must also use very precise measures to detect changes which often are slight. In light of these difficulties, models of the cellular changes underlying learning and memory have been pursued. In studying learning, there are often many nonspecific factors which can influence cellular changes. The accurate localization of responses to electrical stimulation makes it possible to examine very specific neural components contributing to an induced change in the cellular response to stimulation. Long-term potentiation (LTP) is one of the leading in vivo and in vitro models of a possible mammalian storage mechanism at the cellular level. LTP meets many of the physiological and behavioral constraints that define a plausible model system. Some important features of this system are the duration of the enhancement, the occurrence of enhancement in the hippocampus (a structure often implicated in learning and memory), and the fact that LTP is triggered by brief tetani, possibly analogous to the way a brief stimulus event can affect the brain (Squire & Butters, 1984). LTP involves enduring increases in synaptic efficacy in response to high-frequency stimulation. The synaptic alterations associated with LTP are believed to represent the types of synaptic changes that underlie mammalian memory processing; consequently, hippocampal LTP is used as a model through which to explore potential mechanisms of learning and memory. Much of the excitement over LTP concerns the potential for LTP-like changes in synaptic efficacy to underlie processes of mammalian memory storage. There has been gradually increasing support for LTP as a behaviorally relevant type of synaptic plasticity that can be observed following the learning of a behavioral task in the

absence of electrical stimulation. If LTP is a behaviorally relevant phenomenon, it should be observed as a necessary component of behavioral adaptations involving the processing and storage of new information.

LTP is a stable and enduring increase in the magnitude of either the population excitatory postsynaptic potential (EPSP) or the population spike in response to high-frequency tetanizing stimulation (see Figure 1). LTP has been experimentally induced in all pathways of the hippocampal trisynaptic circuit (Figure 2), as well as in many other brain structures (Teyler & DiScenna, 1987). While the pervasiveness of this phenomenon is impressive, the main focus in this paper will be on hippocampal LTP, because of the suggested involvement of the hippocampus in learning and memory processes. LTP can be induced in many areas of the hippocampus, although the magnitude of the synaptic enhancement varies among areas within the hippocampus. Typically, in the dentate the population response following tetanizing stimulation increases in magnitude by 50%-250% over the amplitude of the pre-LTP population spike. The population EPSP, on the other hand, usually demonstrates only a 30-50% increase over the pre-LTP baseline. Generally, in the CA1 region of the hippocampus proper, the EPSP is stronger following LTP than the EPSP of the dentate gyrus given equal stimulus intensity. Similarly, the population spike can be enhanced more reliably in the CA1 region than the population spike in the dentate gyrus.

This synaptic enhancement was first described by Bliss and Lomo (1973) when they observed that following perforant path stimulation to the dentate gyrus in an anesthetized rabbit, there was an enduring increase in the magnitude of the population spike. The increased population spike magnitude varied from 50% to 250% (Figure 3). In a second experiment, Bliss and Gardner-Medwin (1973) reported that increased synaptic efficacy lasts for 16 weeks in unanesthetized rabbits. Because the increased efficacy persisted well beyond the termination of the high-frequency

stimulation trains, this effect may represent a neuronal change useful in information processing and storage.

Many potential mechanisms underlie LTP, and it has not yet been established that LTP involves the same underlying mechanisms across all species and brain structures. In different brain areas, different mechanisms may combine to produce the observed potentiation. Theoretically, LTP may represent increased recruitment of collaterals that previously were not firing, enhanced release of excitatory neurotransmitter, or an increased excitability of the postsynaptic membrane. There may also be morphological changes at the synaptic level involved in the onset of LTP, the maintenance of synaptic efficacy, or both. There is a swelling of spines following LTP (Fifkova & Van Harreveld, 1975), and the shape of the spine can change (Desmond & Levy, 1986). Another morphological correlate of LTP formation was discovered by Lee, Schottler, Oliver, and Lynch (1980), when they found that there was an increase in the number of shaft synapses (see Figure 4) in the in vivo hippocampal CA1 region following the induction of LTP. Lee, Oliver, Schottler, and Lynch (1981) reproduced these findings in an in vitro preparation. Chang and Greenough (1984) looked at the duration of morphological correlates of in vitro hippocampal LTP and found that increased numbers of sessile and shaft synapses lasted up to 8 hours, demonstrating that morphological correlates can exist for the duration of synaptic LTP.

By neurophysiological standards, LTP is an enduring phenomenon. By behavioral standards, if LTP is truly viable as a model for mammalian memory processing, the increased synaptic efficacy should last the full duration of the memory itself. One of the original experiments investigating the behavioral relevance of LTP was performed by Barnes in 1979. The experiment demonstrated that a positive relationship exists between the duration of electrically induced LTP and the level of

ability on a behavioral task. Both mature (10-16 months old) and senescent (28-34 months old) rats were trained on a spatial learning task involving a circular platform. Following training, the rats were administered tetanizing stimulation to the dentate gyrus. The younger rats maintained an enhanced synaptic response for approximately 2 weeks, whereas the aged rats did not sustain any increases in synaptic activity. Furthermore, in the young rats, the amount of synaptic potentiation was strongly correlated with performance ability on the spatial task. These results suggest that an aged nervous system has a decreased capacity for induction and maintenance of synaptic potentiation, which may account for age-related processing deficits.

Behaviorally-induced LTP has been indicated by studies involving the classical conditioning of the rabbit nictitating membrane. Weisz, Clark, Thompson, and Solomon (1982) studied granule cell activity in the dentate gyrus before and during the conditioning of the nictitating membrane response and discovered that changes in synaptic efficacy were consequent to learning the relevance of the tone in predicting the forthcoming airpuff. The tone-airpuff paired group had increased population spikes following tetanizing stimulation, whereas the unpaired animals did not show this increase. Similarly, Skelton, Scarth, Wilke, Miller, and Phillips (1987) demonstrated training-induced synaptic potentiation in the dentate gyrus of rats learning an appetitively motivated operant task. Over an 8 day training period, increased spike amplitudes correlated with task proficiency. This task-induced potentiation was of limited duration, which suggests that it is similar to potentiation induced by electrical stimulation.

In another study investigating the behavioral relevance of long-term synaptic enhancement, Sharp, McNaughton, and Barnes (1985) discovered that dentate gyrus granule cells show increased synaptic activity following exposure to a spatially complex environment. They speculated that in the complex environment, the

potentiated granule cells are involved in the processing of behaviorally relevant spatial information associated with the complexity of the environment. Green and Greenough (1986) performed an *in vitro* study which provided evidence that environmentally-induced synaptic alterations are intrinsic to the hippocampus and disappear when the environmental conditions change. Rats were differentially reared in either enriched environments (EC) or isolated environments (IC) and were then compared for dentate gyrus synaptic response. Initial gains in synaptic efficacy in the EC raised rats were transient and could be reversed if the EC rats were returned to a nonstimulating environment. This experiment was particularly important in that it studied environmentally induced changes in synaptic efficacy *in vitro*, thus isolating the cells from extrahippocampal influences.

The experimental support for increased synaptic efficacy induced by both electrical stimulation and behavioral experience as a model for information processing and storage is thus compelling. The many commonalities suggest that these two processes are not separate phenomena, and may even share underlying neural mechanisms of synaptic enhancement. Regardless of the specific mechanism underlying LTP, it is likely that the increased synaptic efficacy is not solely a neuronal phenomenon, but rather a reflection of changes in many components of the neuropil.

Glia

Despite the important role of neurons in cellular communication, investigators have become increasingly aware that the microenvironment of the central nervous system is extensively populated with glial cells. In the past 20 years, there have been numerous studies highlighting glial cells as modulators of the neuronal environment, and more recently glial plasticity has been acknowledged. In light of all the processing-related changes observed in central nervous system neurons, it may be

that if neuronal elements can respond dynamically to various stimuli, other components of the neuropil are likely to be changing as well.

Although many similarities exist between neurons and glia, some fundamental differences exist that may contribute to their respective roles within the neuropil. To begin with, neurons have axonal processes, and are capable of responding to changes in both intracellular and extracellular ion concentrations by conducting electrical impulses non-decrementally along the length of the axon. Glial cells do not have axons, and their membranes respond passively to electric currents. Neurons and glia differ in their membrane potentials as well. The neuronal membrane responds to changes in K^+ , Cl^- , and Na^+ , and it has a resting potential of -70mv . The glial cell membrane is extremely responsive to changes in K^+ , and it has a resting potential of -90mv , which is determined by the ratio of potassium ions outside the cell to potassium ions inside the cell (Kuffler & Nicholls, 1976). Neuron-glia communication most likely is nonsynaptic, occurring through fluctuations in the extracellular ionic concentrations in the microenvironment, and perhaps a direct transmembrane exchange process, which could occur along the entire length of the neuronal axon. Lastly, glial cells, unlike neurons, can divide throughout the entire life of the organism. These differences are likely to hold the key to understanding the respective roles of these two cell types in information processing.

Glial cells can be divided into five main classes based on differing structure and function. These classes are the microglia, ependymal cells, oligodendrocytes, Schwann cells, and astrocytes. Astrocytes are probably the most relevant in terms of brain plasticity. There are two types of astrocytes, protoplasmic and fibrous astrocytes. Protoplasmic astrocytes have few filamentous processes, and are found abundantly in the gray matter associated with neuronal cell bodies, dendrites, and synapses. Fibrous astrocytes display many filaments and are most often found in the white matter

amongst myelinated axons (Kandel & Schwartz, 1981). At different points in history, every physiological function which could not be experimentally linked to neurons has been attributed to glial cells. However, the actual roles of glial cells are only beginning to be understood. Once described as merely the "glue" holding the neurons together, glial cells now appear to have a much more active role in the neuronal microenvironment .

One proposed function of glial cells is that of nutritive transfer between capillaries and neurons. This hypothesis stemmed from the observation that glial cells have vascular endfeet which attach to capillaries and provide a route for transfer among capillaries, glia, and neurons. Nutritive molecules potentially are internally transported across the glial cell, exiting in an area of close neuronal apposition (Figure 5). Lasek, Gainer, and Przybylski (1974) isolated the giant squid axon and observed that Schwann cells appear to transfer newly synthesized proteins into the axon they envelop. They proposed that a selective macromolecular exchange may occur between neurons and glia. It may also be that if newly synthesized proteins can be transferred from glia to neurons, then a fairly sophisticated and functional communication channel exists between these two cells.

Neurons are not the only cells that respond to alterations in environmental complexity. Glial cells, particularly astrocytes, exhibit plastic changes in response to behavioral experience. Altman and Das (1964) looked at glial cells in rats reared in EC environments and compared them to rats reared in IC environments. By measuring thymidine incorporation, Altman concluded that since EC rats had 60% more thymidine incorporation into nuclear DNA than IC's, the glial cells must be multiplying in the EC rats. Diamond et al. (1966) looked at thionin stained sections of the visual cortex of EC and IC housed rats and found that EC rats had a 14% increase in glial cell numbers, as well as an overall 16% increase in the ratio of glial cells per neuron.

Szeligo and Leblond (1977) examined glial cells in the occipital cortex of young rats raised in an EC, SC, or IC environment postweaning. They measured both cortical thickness and glial cell number changes, and they found that in the EC rats, the occipital cortex increased in both thickness and number of oligodendrocytes and astrocytes. The IC rats did not differ in cortical thickness or glial cell number from the SC rats. Thus, enriching visual and sensory environments can stimulate plastic changes in both neurons and glial cells. The enriching environment accelerated an existing potential for glial cell plasticity and proliferation.

In a recent study, Sirevaag and Greenough (1987) examined the upper four layers of occipital cortex in rats reared for 30 days postweaning in either an EC, SC, or IC environment. This study was an attempt to shed further light on glial cell plasticity in response to differentially complex environments. While the ratio of glial nuclear volume per neuron or synapse was not remarkably different for EC and SC rats, the IC rats had substantially less glial nuclear volume per neuron and synapse. Once again, these findings support the hypothesis that a more efficient and complex nervous system may require more glial volume per neuron to support greater dendritic branching in the EC and SC rats.

Numerous hypotheses have been proposed to explain the presence of increased glial cell numbers in response to complex environmental situations. Glial cells may regulate the neuronal environment by maintaining ionic homeostasis, or modulating the amount of neurotransmitter available to the neuron. They may also be involved in osmoregulation of the neuropil. If EC-raised animals have a more efficient or thorough communication network among neurons, the homeostatic mechanism may be more efficient as well. Glial cell membranes have high permeability to K^+ ions, and consequently are believed to play a role in buffering extracellular K^+ concentrations (Kuffler, Nicholls, & Orkand, 1966). Spatial buffering involves the redistribution of K^+

ions from a region of high potassium concentration to a region of lower concentration. Extracellular K^+ adjacent to firing neurons increases, prompting K^+ influx into astrocytes. An equal amount of K^+ is then thought to exit the astrocyte in an area of lower concentration. The circuit is completed by K^+ returning through the extracellular space.

Newman, Frambach, and Odette (1984) proposed that K^+ redistribution occurs in the retinal Muller cells of salamanders. Spatial buffering activities occurred selectively in the region of the endfoot process. These findings suggest that if this phenomenon can be generalized to astrocytes, then the buffering mechanism may not be merely one of redistributing the K^+ into the nearby extracellular space, but rather the K^+ may be shunted into capillaries where it can be distributed with maximal efficiency. Interestingly, Sirevaag and Greenough (1987) determined that rats raised in an EC environment had larger capillary volume in the occipital cortex in comparison to SC and IC rats, which lends additional support to the hypothesis that glial cells may be involved in a much more sophisticated regulation of the neuronal environment than originally suspected. Neuroglia may maximize the neuronal efficacy by maintaining stability in the neuronal microenvironment.

One way of investigating the role of astroglia in the regulation of extracellular K^+ levels would be to alter the levels of K^+ in the neuronal microenvironment and look for changes in the astrocytes correlating with the environmental changes. Canady, Ali-Osman, and Rubel (1987) plated glial cells from the cerebrum and brain stem of 4-day old hatchling chicks on glass slides in medium containing 5-75 mM KCL, and they processed the slides for immunocytochemical labeling of glial fibrillary acidic protein (GFAP). In cultures with higher concentrations of extracellular K^+ , there was an increase in GFAP immunoreactivity in the astrocytes. Thus, glial cells may swell or proliferate in response to increased concentrations of extracellular K^+ , such as those

that occur adjacent to firing neurons. If this is the case, the glial cells may respond to conditions of enhanced neuronal synaptic efficacy that result from the high-frequency stimulation associated with LTP.

In addition to their role in ionic regulation, glial cells are suspected to respond to osmotic changes in the neuropil. They are also believed to play a role in increasing direct cell-to-cell contact, possibly to facilitate neuronal synchronization during the release of hormones associated with lactation and parturition. Tweedle and Hatton (1976) compared the nucleus circularis and the supraoptic nucleus of normal and water deprived rats and demonstrated that water deprivation brought about a significant increase in cell membrane surfaces in direct contact in both nuclei. Perlmutter, Tweedle, and Hatton (1984) paralleled these findings in a later study looking at the rat supraoptic nucleus. Neurosecretory cells of this nucleus increase their production and release of oxytocin and vasopressin during parturition, lactation, and dehydration. During parturition and lactation there were increased levels of direct apposition of neuronal membranes and formation of double synapses involving a single presynaptic bouton forming two synapses on dendrites. Consistent with earlier findings on water deprived rats (Tweedle & Hatton, 1976), this increased apposition was due to the increased retraction of glial processes. Because a neuronal volume change was not observed to cause the increase in cell contacts, the glial cells presumably were retracting their processes in response to osmotic or blood-borne ionic changes in the neuropil. While the mechanism underlying glial retraction remains unknown, these findings are consistent with the hypothesis that glial cells can respond to changes in the environment to aid in altering functional relationships in the neuropil.

Another way that glial cells could contribute to the efficacy of communication within the neuronal network would be for glial cells to regulate the neurotransmitters used by the surrounding neurons. In a study by Young, Brown, Kelly, and Schon

(1973) using an in vitro preparation, the neurotransmitter gamma-aminobutyric acid (GABA) was selectively taken up by Schwann cells not involved in myelination. They suggested that the glial cells may function in protecting the neurons from excessive amounts of extracellular neurotransmitter. Patterson and Chun (1974) looked at the influence of glial cells on neurotransmitter synthesis in cultures of dissociated sympathetic neurons from a newborn rat and discovered that in the presence of glial cells, the synthesis of acetylcholine was greatly increased. Certain nonneuronal glial cell lines appear to have very selective effects on neurotransmitter synthesis in the presence of neurons.

More recently, Hamberger, Cotman, Sellstrom, and Weiler (1978) suggested that astrocytes aid in regulating the neuronal microenvironment by clearing and storing neurotransmitters used by the synapse. They hypothesize that neuroglia clear glutamate from the synaptic cleft and store its precursor, glutamine. The glutamine can then be returned to the presynaptic terminal to be synthesized into glutamate. These experiments support the hypothesis that glial cells not only exist within the neuropil to support the neuronal communication system, but rather they play an active role in increasing the overall efficiency of the brain by maintaining homeostasis.

Although astrocytes are believed to have many regulatory functions in the neuropil, astroglial ensheathment may also serve as a physical barrier to the formation of synaptic contacts between neurons. Meshul, Seil, and Herndon (1987) used mouse cerebellar explants to demonstrate that astrocytes may play an important role in the regulation of synaptic density. When glial ensheathment was arrested at an early stage of maturation, the cerebellar Purkinje cells showed marked sprouting of axon collaterals. When the explant cultures were transplanted with mature glial cells, there was a 60% reduction in the number of synapses formed along Purkinje cell somata. This experiment demonstrates that glial cell presence may induce changes in

synaptic organization. If astrocytic ensheathment can induce an alteration in the formation of synapses in the hippocampus as well as the cerebellum, then, given that there are lasting increases in numbers of sessile and shaft synapses observed following the induction of hippocampal LTP (Chang & Greenough, 1984), there may be a change in astrocytic surface density following the induction of LTP.

The question that still needs to be answered is, "How do the glial cells respond during information processing?" There are a variety of approaches to answering this question, one of which is looking at how the glial cells react to neurons that are actively firing at maximum levels. It is probable that glial cells respond to this type of situation, but there are many different ways in which they can change. They can increase in size or number; they can reach out to more thoroughly ensheath the neuron, or they can retract their processes to allow for increased neuron-neuron apposition or synaptic formation. Any of these changes would represent glial plasticity in response to neuronal changes.

One question that has not been experimentally addressed concerns glial adaptation during neuronal long-term potentiation. If LTP is a model for neuronal information processing, and if glial cells have a role in this processing, then glial plasticity should be evident in response to synaptic enhancement. The research question I am investigating is whether or not there is a change in the surface density or thickness of astrocytic processes in the dentate gyrus molecular layer following synaptic potentiation. Given the many functions of glia, and the numerous experiments demonstrating the ability for glial cells to respond to environmental alterations, it is plausible that glial cells will respond to the altered cellular environment accompanying synaptic potentiation.

Methods

Part 1: Baseline Surface Density and Thickness of Astrocytic Processes in the Dentate Gyrus and CA1 Regions of the Hippocampal Formation

Subjects

Six male Long-Evans hooded rats (Simonsen stock), 80-90 days old, that had been socially housed (two rats per cage) up to the time of perfusion were used. The rats were anesthetized with sodium pentobarbital and then perfused through the heart with 50 ml of 0.1 M phosphate buffer (PB, pH 7.4) followed by 50 ml of 4% paraformaldehyde and 0.08% glutaraldehyde in saturated picric acid buffered to pH 7.4. The cerebella were removed and the brains remained in the fixative for one hour. The frontal lobes were also removed in order to isolate the brain area of interest (hippocampal formation) and to allow fixative penetration. The tissue was subsequently transferred to a glutaraldehyde-free fixative for six hours. The tissue was then washed in a 30% sucrose cryoprotection solution overnight and frozen in liquid nitrogen the following day. Coronal sections of eight microns (μm) were cut on a cryostat and immunocytochemically processed for glial fibrillary acidic protein (GFAP).

Tissue Processing

An indirect immunocytochemical procedure using an avidin-biotin complex (ABC) labeled with peroxidase was used to visualize astrocytes in the hippocampal dentate gyrus and CA1 region (Figure 6). After sections were cut and air dried, the sections were washed in PB and blocked with a 10% normal donkey serum to avoid non-specific antibody binding. The serum contained .5% Triton X-100 as a detergent that disrupts the tissue and facilitates antibody penetration. The tissue was incubated overnight in a 1:400 dilution of primary antibody (mouse anti-GFAP, ICN labs), and was washed 6x10 minutes in PB the next morning. Next the sections were incubated in a 1:100 dilution of the secondary antibody (biotinylated anti-mouse IgG, Vector labs)

for two hours at room temperature and four degrees overnight. The following morning the tissue was washed 6x10 minutes in PB and incubated with an ABC reagent (Biomedica) containing peroxidase for two hours at room temperature. After the slides were washed, the peroxidase reaction was completed by exposure to .01% diaminobenzidine (DAB) in a nickel ammonium sulfate solution to enhance the reaction. The slides were then washed before coverslipping with permount. This indirect method of staining involves first applying a primary monoclonal antibody, which binds to GFAP, and second applying a biotinylated secondary antibody which binds to the primary antibody as the antigen. Next, the avidin-biotin complex is added, in which the avidin molecule (a large glycoprotein from egg white) has a proportion of its biotin (a vitamin with a high affinity for avidin) sites free to react with the biotinylated secondary antibody. The biotin complex is labeled with peroxidase, an enzyme which is visualized by allowing it to oxidize diaminobenzidine (DAB). This layering method provides strongly stained tissue sections with a visible end product of darkly stained astrocytic processes suitable for cycloid analysis.

Quantitative Analysis

Surface density of astrocytic processes. For each animal, an area of 129,168 μm^2 per subject was sampled in the dentate gyrus and 129,168 μm^2 in the CA1 region, viewed under a 100X objective on an Olympus BH-2 microscope. The surface density (S_v) of GFAP-positive astrocytic processes was estimated using the stereologically unbiased cycloid grid method (Baddeley, Gundersen, & Cruz-Orivet, 1986). S_v is equal to the surface area per unit volume of tissue. The cycloid method for estimating S_v uses a test frame of cycloid curves (Figure 7), and the total number of astrocytic processes intersecting the cycloid curves while focusing through the tissue gives an unbiased estimate of surface area. Stereological procedures involve mathematical methods that relate two-dimensional measurements obtained on sections

to three-dimensional parameters of astrocytic processes and somas (Weibel, 1979). The standard methods of stereology assume that uniformly random samples (IUR) are taken to provide an unbiased sample. IUR samples are difficult to obtain when taking hippocampal coronal sections, but the use of the cycloid grid compensates for the violation of the IUR assumption. The cycloid frame was superimposed on each 8 μm section through the eyepiece of the microscope, and the vertical axis of the frame was consistently aligned with the vertical orientation of the section. The number of intersections of cycloid arcs and astrocytic processes was counted, and S_v was calculated using the following formula:

$$S_v = 2(P/L)(\Sigma I/\Sigma P)$$

where I was the number of intersections of arcs and processes, and P was the number of test points which fell in the sample space. (P/L) was a conversion factor to real units where P was the number of test points and L was the length of a single cycloid arc multiplied by the number of cycloids in the grid (Baddeley et al., 1986).

Thickness of astrocytic processes. For approximately every third intersection of a cycloid arc and an astrocytic process, the thickness of the process was estimated. A computer was programmed to beep randomly on the average of every third intersection counted, and when the beep was heard, the thickness of that process was recorded on a scale from 1 to 5, where 1=less than 1 μm , 2=.75 to 1.0 μm , 3=1.5 to 1.75 μm , 4=2.0 to 3.0 μm , and 5= a process thickness greater than 3.5 μm .

Part 2: Effect of LTP Induction In Vivo on Astrocytic Process Size and Density in the Hippocampal Dentate Gyrus

Subjects

10 male Long-Evans hooded rats (Simonsen stock), 90-120 days old, that had been socially housed (two rats per cage) up to the beginning of the experiment were used.

Treatment

Teflon-coated stainless electrodes (110 μm in diameter) were implanted in equivalently aged animals on the same day or within 24 hours into the dentate gyrus hilar region (coordinates: 3.8 mm posterior to Bregma and 2.0 mm lateral to midline) and in the angular bundle of the perforant path (coordinates: 8.1 mm posterior to Bregma and 4.4 mm lateral to midline). Approximately 500 μm of insulation was scraped off the bipolar stimulating electrode during implantation. Only one penetration of each electrode was made, in order to ensure correct localization of the electrode track when making estimates of the section distance anterior or posterior to the electrode tip. The electrodes were then cemented into place with dental acrylic.

We waited 4-6 weeks to allow adequate time for recovery from surgery before placing the rat in the recording chamber. We then waited 20 minutes to allow the rat time to become accustomed to the chamber before conducting an input/output (I/O) curve (stimulus range varied depending on the animal; usually between 80 μA and 800 μA) on the rat beginning at the first sizeable population evoked potential and ending when a consistent plateau was reached. After conducting the I/O curve, we took a baseline sweep at approximately one-third of the maximal spike height.

We next selected each rat to be in either the activity control (AC) or long-term potentiation (LTP) condition by the process of assigning the rat with the larger baseline response from the first pair to the LTP condition, and the rat with the larger response from the second pair to the AC condition, and so on, to avoid the chance that all the rats with the greater baseline response were placed in the same group. For the LTP subjects, we administered stimulus trains at the maximum intensity derived from the I/O curve at 400 Hz (10 pulses/train, 10 trains/minute, duration: 1 minute). After 30 minutes, we reset to the original baseline sweep stimulation parameters, and collected a second sweep which we compared with the baseline sweep. For the AC

condition, we gave equivalent amounts of stimulation (100 pulses: one pulse every 6 seconds (.167 Hz) for 10 minutes) at the intensity which elicited a maximal spike response as derived from the I/O curve. We then waited for 30 minutes before collecting a test sweep at the same intensity as the baseline sweep to confirm the absence of LTP. We next conducted an I/O curve on the animals in both conditions at the same settings as prior to stimulation in order to examine responses across a range of stimulation intensities. 24 hours later, we checked for LTP by placing the animal in the chamber again, waiting 20 minutes, and conducting a third test sweep and I/O curve at the original settings. After confirming the existence of LTP or lack thereof in the AC rats, we perfused the animals and stained the sections with a monoclonal anti-GFAP antibody (Biogenex labs).

Tissue Preparation

The perfusion and immunocytochemical procedures used in this experiment were identical to those used in experiment 1. For this second experiment, a section thickness of 10 μ m was used.

Quantitative Analysis

The LTP and AC condition rats were matched on the basis of the length of time of electrode implantation as well as date of birth. The cycloid grid method described for experiment 1 was used to estimate the Sv of astrocytic processes in the hippocampal dentate gyrus at four different distances on a rostral-caudal axis from the electrode tip (80 to 120 μ m, 180 to 220 μ m, 280 to 320 μ m, and 380 to 420 μ m) in order to measure the interaction between distance from the electrode tip as an indication of damage-induced gliosis and LTP effect outside the zone of gliosis for the LTP and AC conditions. We also estimated the thickness of the astrocytic processes for both

conditions at different distances from the electrode tip using the same method as described for experiment 1.

Results

Part 1: Astrocytic Surface Density and Process Thickness Analysis

Astrocytic surface density (S_v) in the hippocampal dentate gyrus molecular layer was quantified using the method of Baddeley et al. (1986), which provides an unbiased estimate of astrocytic surface density. The molecular layer was divided into three sections, where the first division corresponded to the outermost third of the molecular layer, the second to the middle third, and the inner division to the area just above the granule cell layer. The density and size of astrocytic processes delineate the functional sublamination of the dentate gyrus molecular layer with regard to its afferents. A total area of $129,168 \mu\text{m}^2$ per subject was sampled, and approximately 900 processes were sampled per animal from each of the three divisions of the molecular layer. The ANOVA ($F=165.79$, $p<.0001$) showed that there was a significant difference in surface density across thirds (outer $S_v=14.58$, middle $S_v=11.54$, inner $S_v=8.37$). The Student Neuman-Keuls comparisons indicated that S_v in all thirds were different from each other ($p<.01$). Astrocytic surface density is highest in the outer third of the molecular layer and progressively decreases as one approaches the granule cell layer (see Figure 8).

Astrocytic surface density in the stratum radiatum of the hippocampal CA1 region was quantified using the same method as above (see Figure 9). The stratum radiatum was divided into thirds, and the three samples were not statistically different (proximal $S_v=13.85$, middle $S_v=13.74$, inner $S_v=13.79$; $p>.05$ for the ANOVA, $F=0.19$).

Astrocytic process thickness in the dentate molecular layer was estimated based on a scale from 1-5 where 1= $<.5 \mu\text{m}$, 2= $.75-1.0 \mu\text{m}$, 3= $1.5-1.75 \mu\text{m}$, 4= $2.0-3.0 \mu\text{m}$, and 5= $>3.5 \mu\text{m}$. The molecular layer was divided into thirds for the analysis of the relative

frequency of process thicknesses. Astrocytic process thickness decreases , on the average, as one moves from the outer third of the molecular layer to the innermost third (see Figure 10). The Kolmogorov-Smirnov tests confirmed all three distributions of thickness to be different ($p < .01$), and separate ANOVAs for each size category showed that the relative frequencies of astrocytic process sizes were statistically different across the thirds of the dentate gyrus molecular layer ($p < .01$).

Part 2: LTP Effect on Astrocytic Surface Density and Process Thickness Analysis

Percentage of long-term potentiation (LTP) was measured 24 hours after the last LTP train was administered. The population spike area was measured from a sweep collected at an intensity which generated a spike of approximately one-third of the maximal spike height prior to stimulation. On average, LTP rats showed an increase in population spike area of 113.44% and activity control (AC) rats showed an increase of 26.17%.

Astrocytic surface density (Sv) and process thickness was examined at 4 different distances from the tip of the recording electrode (100 μm , 200 μm , 300 μm , and 400 μm) to measure the effect of LTP or AC stimulation on glial cells and in order to detect a possible interaction between treatment and distance from the electrode tip as an indication of damage-induced gliosis. In some analyses, processes of thickness 3, 4, and 5 were analyzed as a group to assess trends that were typically evident across the categories. In all cases processes of category 4 and category 5 were grouped for at least one analysis due to their relatively small numbers. When the Sv data was analyzed by group for evidence of gliosis (increased glial tissue), the LTP rats showed increases in Sv at 100 and 200 μm when compared to Sv values measured at distances of 300 and 400 μm ($F=2.73$, $p < .05$). AC rats exhibited increases in Sv at 100, 200, and 300 μm when compared to Sv values measured at 400 μm from the electrode tip ($F=3.58$, $p < .02$). In both treatment groups, the processes showing the

greatest change at different distances from the electrode track are processes of thickness 1 (Student Neuman-Keuls test, $p < .05$).

At 100 μm from the recording electrode tip there were no significant differences in Sv between the LTP and the AC groups when analyzed across all thirds of the molecular layer as shown in Figure 11 ($F = 0.19$, $p > .05$). Astrocytic Sv was quantified using the same method as described for part 1 of this experiment, and astrocytic process thickness was estimated using the same method and scale described for part 1 of this experiment. As shown in Figure 12, when analyzed both across and within thirds of the molecular layer, there were significant differences in the frequency of processes of thicknesses 1 and 2 between the LTP and the AC groups ($F = 6.49$, $p < .01$). In the middle third of the molecular layer there was a significant increase (18%) in the frequency of processes of thickness 1 in the LTP group ($F = 7.75$, $p < .01$), and in the outer third there was a significant increase (42%) in processes of thickness 2 in the LTP group ($F = 8.32$, $p < .01$). There were no significant differences in the frequency of process thicknesses of 3, 4, and 5 when analyzed across layers or when analyzed by layers.

When Sv was analyzed at 200 μm from the electrode tip, despite the fact that the LTP group was greater than the AC group in all thirds of the molecular layer, this difference failed to reach acceptable levels of significance ($F = 3.11$, $p < .08$, see Figure 13). When analyzed across thirds, the frequency of processes of thicknesses 3, 4, and 5 was significantly greater for the LTP group ($F = 34.09$, $p < .0001$). For the LTP group, the frequency of processes of thickness 3 was 95% greater than the AC group, and the frequency of processes of thickness 4 and 5 combined was 81% greater than the AC group. As shown in Figure 14, when analyzed by thirds of the molecular layer, in the outer layer the frequency of processes of thicknesses 4 and 5 combined was significantly greater for the LTP group than the AC group ($F = 10.09$, $p < .01$). The

frequency of processes of thickness 3 was also significantly greater for the LTP group ($F=7.27$, $p<.02$). For the middle third of the molecular layer, processes of thicknesses 4 and 5 combined showed a trend toward greater frequencies in the LTP group ($F=2.06$, $p<.2$), and processes of thickness 3 were significantly greater in the LTP group than the AC group ($F=21.17$, $p<.001$). For the inner third of the molecular layer, the frequency of processes of thickness 3 was significantly greater in the LTP group ($F=10.54$, $p<.01$). In regards to processes of thicknesses 1 and 2, across the layers the frequency of 2's was 29% greater in the LTP condition than the AC condition ($F=35.23$, $p<.0001$), and the frequency of processes of thickness 1 was 32% greater in the AC condition than the LTP condition ($F=4.37$, $p<.04$).

As shown in Figure 15, at 300 μm from the electrode tip, there were no statistically significant differences in Sv between the LTP and the AC groups when analyzed across all thirds ($F=0.05$, $p>.05$). For the analysis of process thickness, large coefficients of variation appeared to result from inconsistencies in both the immunocytochemical staining and the tissue preparation. Consequently, there were no detectable significant differences found at 300 μm from the electrode tip ($p>.05$ for all comparisons).

As shown in Figure 16, at 400 μm from the electrode tip the astrocytic Sv was significantly greater for the LTP condition than the AC condition when analyzed across all thirds of the molecular layer ($F=4.66$, $p<.05$). The LTP group had greater frequencies of processes of thicknesses 3, 4, and 5 when analyzed across all thirds of the molecular layer ($F=8.74$, $p<.01$). As shown in Figure 17, when analyzed by thirds of the molecular layer, the outer third shows a trend toward increased frequencies of processes of thicknesses 4 and 5 combined for the LTP group. In the middle third of the molecular layer, processes of thicknesses 4 and 5 combined are found at significantly greater frequencies in the LTP group ($F=4.92$, $p<.05$). In the inner third of

the molecular layer, the frequencies of processes of thicknesses 3, 4, and 5 are significantly greater for the LTP group ($F=4.58$, $p<.05$). The frequency of processes of thickness 3 is 26% greater for the LTP group, and the frequency of 4's and 5's combined is 52% greater for the LTP group than the AC group when analyzed across thirds of the molecular layer. When analyzed across thirds and when analyzed by thirds, there were no significant differences in the frequencies of processes of thicknesses 1 and 2 combined between the LTP and the AC groups ($F=0.5$).

Discussion

In part 1 of our experiment we examined the surface density and thickness of astrocytic processes in the outer, middle, and inner thirds of the hippocampal dentate gyrus. This investigation revealed that the density and size of astrocytic processes delineate the functional sublamination of the dentate gyrus molecular layer with regard to its afferents, the lateral and medial perforant paths and the commissural and associational fibers. Astrocytic surface density is highest in the outer third of the molecular layer and progressively decreases in the middle and inner thirds as one approaches the granule cell layer. In addition, astrocytic process thickness decreases, on average, as one moves from the outer third of the molecular layer to the innermost third. Lastly, there was no equivalent regional differentiation evident within stratum radiatum of the CA1 region of the hippocampus. Together, these results indicate that in the hippocampal dentate gyrus the distribution and size of astroglial processes is different for all thirds of the molecular layer in animals receiving no experimental treatment.

The distribution of astrocytes in the molecular layer of the dentate gyrus was examined previously by Kishi, Stanfield, and Cowan (1978). These investigators studied gold chloride-sublimate preparations from both rats and mice. In agreement with our results, they concluded that the density of astrocytes was relatively low within

the zone of termination of the commissural and associational connections to the dentate gyrus (i.e., the innermost layer). Kishi et al. (1978), report an aggregation of astrocytic cell bodies near the pial surface that corresponds to our outermost layer. Generally, thicker processes are found mostly near cell bodies, which explains why there may be more processes of thicknesses 4 and 5 in the outer third of the molecular layer. For the inner and middle thirds of the molecular layer, the astrocytic cell bodies were found to be randomly scattered with no distinguishable pattern. This may explain the presence of some processes of thicknesses 4 and 5 in the inner and middle thirds of the molecular layer.

More recently, Kosaka and Hama (1986) used Golgi-impregnated sections to study the three dimensional structural details of protoplasmic astrocytes of the dentate gyrus. They classified astrocytes into six subtypes based on the location of their somata within the dentate gyrus. In the inner portion of the molecular layer, the astrocytes were stellate in shape, radiating their processes in all directions. In the outer portion of the molecular layer, the astrocytes were elongated and extended their long, straight processes radially. Astrocytes in the subgranular zone were of the radial type, and extended their processes into the granule cell layer. At the border of the molecular and granule cell layer, the astrocytes appeared to be upside-down radial astrocytes, and beneath the pial surface many astrocytes extended their processes into the molecular layer. These observations reveal that many of the processes observed in the molecular layer may originate in another layer and extend their processes up through the granule cell layer and into the molecular layer.

Part 2 of this experiment was designed to determine the effect of LTP induction in vivo on astrocytic process size and density in the molecular layer of the hippocampal dentate gyrus. It was hypothesized that the increased physiological activity due to the induction of LTP should have some effect on glial processes, which are responsible for

maintaining the extracellular environment and processing some neurotransmitter metabolites. We found an increase in the surface density of glial processes at 400 μ m from the tip of the recording electrode 24 hours following the administration of potentiating stimulus trains. At 400 μ m there were more thicker processes, but no reduction in thinner processes. This would suggest that there may be both swelling of existing processes and the production of new thinner processes to replace the processes that have swollen. Alternatively, some of the thicker processes may have swollen and new branch buds (fairly thick) were being produced at the same time. Astrogliosis was evident within 300 μ m of the electrode track, but at a distance of 400 μ m damage-induced gliosis did not appear to occur. Together, these results indicate that at a distance of 400 μ m from the electrode track there are increases in the surface density and size of astrocytic processes in the LTP group that are not found in the AC group and that are not induced by electrode penetration.

Part 2 of this experiment was designed to determine the types of glial adaptations that may accompany neuronal long-term potentiation. During hippocampal LTP, the potentiated neurons are believed to be firing at maximal levels. Desmond and Levy (1988) reported neuronal anatomical correlates of synaptic potentiation for the middle third of the dentate molecular layer. They stated that while many anatomical synaptic changes accompany long-term potentiation, synaptogenesis was not evident. The anatomical changes reported included an increased incidence of concave dendritic spine heads, an increased surface area of spine heads, an increased postsynaptic density area of spine heads, wider dendritic spine stems, and an increase in the number of synaptic vesicles evident in the presynaptic terminals. These results indicated that the synaptic changes accompanying LTP may represent changes in the strength of the existing synapses. Given that neuronal elements can respond dynamically to potentiating stimulation, and knowing that the neuronal environment is

extensively populated with glial cells, it is not unreasonable to suppose that glial components are changing in accord with, or in response to, these synaptic strength changes.

Essentially, there are two ways that glial cells could respond to the neuronal and synaptic alterations observed following the administration of potentiating stimulation. Glial cells may retract their processes to allow for increased neuronal apposition, synchronization, and synaptic connectivity. Alternatively, the glial processes may increase in size and number in order to more efficiently regulate the changing ionic and osmotic microenvironment of the neuropil which may accompany synaptic potentiation. Additionally, glial adaptations may vary depending on the specificity of glial function and glia-neuron interactions within a particular brain region.

Tweedle and Hatton (1976) demonstrated that increases in direct neuron-neuron apposition in the nucleus circularis and the supraoptic nucleus following water deprivation were due to an increased retraction of glial processes in the neuronal environment. Tweedle and Hatton (1984) paralleled these findings in a later study that demonstrated increased levels of direct apposition of neuronal membranes during parturition and lactation in the rat supraoptic nucleus. Consistent with these earlier findings, Modney and Hatton (1988) demonstrated that comparisons made between the supraoptic nuclei of dehydrated and control rats revealed increases in somatic/dendritic membrane apposition and formation of double synapses. While the mechanism of glial retraction remains unknown, presumably the glial cells are responding to ionic or osmotic changes in the neuropil associated with the altered demands accompanying dehydration, lactation, and parturition.

While glial retraction has been observed in certain areas of the brain following experimental manipulations, other investigators have demonstrated that glial cells may become swollen following experimental treatment. Wolff and Guldner (1978)

unilaterally stimulated the optic nerves of anesthetized albino rats and found that in the visual cortex of stimulated rats, swollen astrocytic processes appeared in close proximity to axo-dendritic synapses. Although the unilateral stimulation produced effects in both hemispheres, the density of swollen processes was highest in the ipsilateral cortex. Interestingly, the observed swelling represented an increase in volume accompanied by a retraction of the smaller, finger-like lamellar processes. The observed astrocytic swellings were heterogeneously distributed, with some regions essentially devoid of swollen processes. This experiment provides evidence that changes in neuronal activity prompted by electrical stimulation may induce structural changes specifically in astrocytic processes located near synaptic terminals.

Evidence has shown that changes in glial processes may occur rapidly in response to changes in neuronal activity, and that temporal factors are important to consider when studying glial plasticity. Edwin Rubel (personal communication, March 14, 1989) noticed an increase in glial process growth within 30 minutes following the cessation of neuronal activity in the nucleus magnocellularis. After 2 hours, there was a 40% increase in GFAP staining of astrocytic processes. After 6 hours, there was an 80-100% increase observed in GFAP staining. The use of light microscopy confirmed that the increase in GFAP staining was not due to glial proliferation or polymerization, but rather was due to an increase in the number of glial processes. Following termination of neuronal activity, the glial cells appeared to wrap around and more thoroughly ensheath neuronal components. Interestingly, upon later stimulation of these neurons, glial retraction was observed. Essentially, this experiment demonstrates that rapid cytochemical changes may take place in glia following interruption of presynaptic input. These results contrast with ours in that we observed glial swelling and extension in response to increased neurophysiological activity.

These discrepant results may be due to the fact that glial functions may be different in different brain areas or that different experimental time courses were used.

Glial cell plasticity in response to differential levels of environmental experience was examined by Sirevaag and Greenough (1987) for the upper 4 layers of the occipital cortex in rats reared in complex (EC), social (SC) or individual cage (IC) environments. It was found that rats reared in the IC environment had significantly less glial nuclear volume per neuron and synapse than rats reared in EC or SC environments. In addition, the mean astrocytic nuclear volume was greater in EC rats than SC or IC rats. Essentially, rats reared in more complex environments had more glial support per neuron than rats reared in IC environments. These results are compatible with the hypothesis that glial cells may have a role in regulating the metabolic efficacy of the central nervous system communication network, and therefore a more efficient cellular network may demand increased glial support.

Glial plasticity has also been demonstrated in response to other types of environmental alterations. Jaeger (1988) demonstrated that astrocytes have the capacity to alter the length of their processes in vivo in response to implantation of a foreign object into the cellular environment. Nitrocellulose filters were cografted with PC12 cells such that the filters provided a substrate for the astrocytes, and the PC12 cells provided a growing matrix. The astroglia formed contacts with the filter during the initial stages of cograft placement, and when the PC12 cell graft enlarged due to cell division, the glial cells that were anchored in the filter and attached at the other end to adjacent glia or capillaries elongated their processes in response to the force exerted by the surrounding growing tissue. This glial "stretching" was observed in GFAP-positive glial cells and resulted in processes that were 2 to 5 times longer than those of other astrocytes. From this evidence, it appears that glial cells may alter their shape and orientation in response to environmental alterations.

Denis-Donini, Glowinski, and Prochiantz (1984) reported that *in vitro*, glial cells may exert a morphogenetic effect on dopaminergic neurons. When mesencephalic dopaminergic neurons were plated onto glial cells from the mesencephalon, the neurons developed extensive neurite outgrowths, suggesting that glial cells can alter the morphology of neurons.

In studying changes in astrocytic processes in response to alterations in the central nervous system microenvironment, damage-induced gliosis (increased glial tissue) must be taken into consideration. Gage, Olejniczak, and Armstrong (1988) showed that damage to the fimbria-fornix and separately to the perforant path prompted temporal changes in astrocytes located in the dentate molecular layer. Following fimbria-fornix lesions, there were selective increases in dentate gyrus astrocytic immunoreactivity in the inner portion of the molecular layer, and following perforant path lesions there were selective increases in astrocytic immunoreactivity in the outer portion of the molecular layer. The observed changes disappeared 30 days postlesion. Given that astrocytes are hypothesized to be involved in many types of nutritive and metabolic neuronal support, astrocytes may proliferate near areas of terminal degeneration in order to support neurite outgrowth and dendritic sprouting responses in damaged neurons.

Aebischer, Winn, and Galletti (1988) inserted polymer capsules into the rat parietal cortex parenchyma and observed GFAP-labeled reactive astrocytes at distances less than 400 μ m from the polymer capsules during the first two weeks postimplantation. By 12 weeks postimplantation, the reactive zone had greatly diminished and immunoreactive astrocytes were observed only in close apposition to the polymer membrane material. Our results are consistent with these observations; in the LTP rats, increases in surface density at 100 μ m and 200 μ m from the electrode track were observed in comparison to 300 μ m and 400 μ m from the electrode track. For

the AC rats, increases in surface density were observed up to 300 μ m from the electrode tip in comparison to 400 μ m. Together, these observations indicate that while there may have been an interaction between experimental treatment effects and reactive gliosis at distances less than 300 μ m from the electrode track, the increases in surface density and process thickness observed in LTP animals 400 μ m from the electrode tract are not due to damage-induced reactive gliosis.

Although evidence for both glial retraction and glial swelling has been presented here, our results are most consistent with the hypothesis that glial processes increase in density and thickness in the environment of potentiated neurons. These findings are not surprising given the many hypothesized functions of glial cells in the metabolic, ionic, and osmotic regulation of the microenvironment of the central nervous system. Glial cells are believed to be involved in nutritive support of neurons (Lasak et al., 1974), K⁺ regulation (Kuffler et al., 1966), and Cl⁻ regulation (Bourke, Kimbler, & Nelson, 1976). In addition, astrocytes appear to be involved in neurotransmitter synthesis (Patterson & Chun, 1974), and storage (Hamberger et al., 1978).

In summary, our experimental results provide evidence that there are distinct differences in astrocytic surface density and process thickness among thirds of the dentate gyrus molecular layer, and that this distribution changes following the administration of LTP-inducing tetanizing stimulation. Despite much convincing evidence that both glial and neuronal components can respond dynamically to alterations in the cellular environment, one question that still needs to be addressed concerns the temporal relations between neuronal and glial changes. On the one hand, it may be that neurons respond primarily to changes in levels of neuronal stimulation, and the glial cells subsequently respond to the neuronal changes. An example of this sequence of events would be an increase in glial size and numbers in response to the greater metabolic demands of neurons firing at maximal levels. On the

other hand, it may be that glial cells respond initially, and neuronal changes occur following glial responses to presynaptic firing rates. An example of this sequence of events might be a retraction of glial processes in response to ionic or blood-borne osmotic changes in the neuropil, followed by neuronal synaptogenesis or morphological changes in the space vacated by the glial process retraction. A third alternative is that the neuronal and glial components change simultaneously or in a complicated sequence. Future experiments will attempt to delineate the time course of the glial response in concert with an examination of the neuronal response to stimulation.

Bibliography

- Aebischer, P., Winn, S.R., & Galletti, P.M. (1988). Transplantation of neural tissue in polymer capsules. Brain Research, 448, 364-368.
- Altman, J. & Das, G.D. (1984). Autoradiographic examination of the effects of enriched environment on the rate of glial multiplication in the adult rat brain. Nature, 204, 1161-1163.
- Baddeley, A.J., Gundersen, H.J.G., & Cruz-Orivet, L.M. (1986). Journal of Microscopy, i42, 259-276.
- Barnes, C.A. (1979). Memory deficits associated with senescence: A neurophysiological and behavioral study in the rat. Journal of Comparative Physiological Psychology, 93, 74-104.
- Bliss, T.V.P., & Gardner-Medwin, A.R. (1973). Long-lasting potentiation of synaptic transmission in the dentate area of the unanaesthetized rabbit following stimulation of the perforant path. Journal of Physiology, 232, 357-374.
- Bliss, T.V.P., & Lomo, T. (1973). Long-lasting potentiation of synaptic transmission in the dentate area of the anaesthetized rabbit following stimulation of the perforant path. Journal of Physiology, 232, 331-356.
- Bourke, R.S., Kimbler, H.K., and Nelson, L.R. (1976). The effects of temperature and inhibitors on HCO₃ stimulated swelling and ion uptake of monkey cerebral cortex. Brain Research, 105, 309.
- Chang, F.-L.F., & Greenough, W.T. (1982). Lateralized effects of monocular training on dendritic branching in adult split-brain rats. Brain Research, 232, 283-292.
- Chang, F.-L.F., & Greenough, W.T. (1984). Transient and enduring morphological correlates of synaptic activity and efficacy change in the rat hippocampal slice. Brain Research, 309, 35-46.

- Cohen, L. (1958). Sherrington: Physiologist, philosopher, and poet. Liverpool, Great Britain: Eaton Press.
- Denis-Donini, S., Glowinski, J., and Prochiantz, A. (1984). Glial heterogeneity may define the three-dimensional shape of mouse mesencephalic dopaminergic neurons. Nature, **307**, 641-643.
- Desmond, N.L., & Levy, W.B. (1986). Changes in post-synaptic density with long-term potentiation in the dentate gyrus. Journal of Comparative Neurology, **253**, 476-482.
- Desmond, N.L., & Levy, W.B. (1988). Anatomy of associative long-term synaptic modification. In P.W. Landfield & S.A. Deadwyler (Eds.), Long-term Potentiation: From Biophysics to Behavior (pp. 265-305). New York: Alan R. Liss.
- Diamond, M.C., Law, F., Rhodes, H., Linder, B., Rosenzweig, M.R., Krech, D., & Bennett, E.L. (1966). Increases in cortical depth and glial numbers in rats subjected to enriched environment. Journal of Comparative Neurology, **128**, 117-126.
- Fifkova, E., & Van Harreveld, A. (1975). Swelling of dendritic spines in the fascia dentata after stimulation of the perforant path fibers as a mechanism of post-tetanic potentiation. Experimental Neurology, **49**, 736-749.
- Gage, F.H., Olejniczak, P., & Armstrong, D.M. (1988). Astrocytes are important for sprouting in the septohippocampal circuit. Experimental Neurology, **102**, 2-13.
- Green, E.J., & Greenough, W.T. (1986). Altered synaptic transmission in dentate gyrus of rats reared in complex environments: Evidence from hippocampal slices maintained *in vitro*. Journal of Neurophysiology, **55**, 739-750.
- Green, E.J., Greenough, W.T., & Schlumpf, B.E. (1983). Effects of complex or isolated environments on cortical dendrites of middle-aged rats. Brain Research, **264**, 233-240.

- Greenough, W.T., & Volkmar, F.R. (1973). Pattern of dendritic branching in occipital cortex of rats reared in complex environments. Experimental Neurology, 52, 372-383.
- Hamberger, A., Cotman, C.W., Sellstrom, A., & Weller, T. (1978). Glial cells and their relationship to transmitter glutamate. In Scoffenells, E., Frank, G., Towers, D.B., & Hertz, L. (Eds.), Dynamic properties of glial cells. Oxford: Pergamon Press.
- Hebb, D.O. (1949). The organization of behavior. New York: Wiley.
- Jaeger, C.B. (1988). Plasticity of astroglia: Evidence supporting process elongation by "stretch". Glia, 1, 31-38.
- Juraska, J.M., Fitch, J.M., Henderson, C., & Rivers, N. (1985). Sex differences in the dendritic branching of dentate granule cells following differential experience. Brain Research, 333, 73-80.
- Kandel, E.R., & Schwartz, J.H. (Eds.). (1981). Principles of neural science. New York: Elsevier North Holland.
- Kishi, K., Stanfield, B.B., & Cowan, W.M. (1978). A note on the distribution of glial cells in the molecular layer of the dentate gyrus. Brain Research Bulletin, 4, 35-41.
- Kosaka, T., & Hama, K. (1986). Three-dimensional structure of astrocytes in the rat dentate gyrus. Journal of Comparative Neurology, 249, 242-260.
- Kuffler, S.W., & Nicholls, J.G. (1976). From neuron to brain: A cellular approach to the function of the nervous system. Sunderland, MA: Sinauer.
- Kuffler, S.W., Nicholls, J.G., & Orkand, R.K. (1966). Physiological properties of glial cells in the central nervous system of amphibia. Journal of Neurophysiology, 29, 768-787.
- Lasek, R.J., Galner, H., & Przybylski, R.J. (1974). Transfer of newly synthesized proteins from Schwann cells to the squid giant axon. Proceedings of the National Academy of Sciences, 71(4), 1188-1192.

- Lee, K.S., Oliver, M., Schottler, F., & Lynch, G. (1981). Electronmicroscopic studies of brain slices: The effects of high-frequency stimulation on dendritic ultrastructure. In Kerkut, G.A., & Wheal, H.V. (Eds.), Electrophysiology of Isolated Mammalian CNS Preparations. New York: Academic Press.
- Lee, K.S., Schottler, F., Oliver, M., & Lynch, G. (1980). Brief bursts of high-frequency stimulation produce two types of structural change in rat hippocampus. Journal of Neurophysiology, 44, 247-258.
- Meshul, C.K., Sell, F.J., Herndon, R.M. (1987). Astrocytes play a role in regulation of synaptic density. Brain Research, 402, 139-145.
- Modney, B.K., & Hatton, G.I. (1988). Dehydration induced increases in rat supraoptic neuronal cell size is accompanied by absolute increases in multiple synapses, neuronal membrane apposition and glial contact. (From Psychological Abstracts, 1988, Abstract No. 454.10).
- Newman, E.A., Frambach, D.A., & Odette, L.L. (1984). Control of extracellular potassium levels by retinal glial cell K⁺ siphoning. Science, 225, 1174-1175.
- Patterson, P.H., & Chun, L.L. (1974). The influence of non-neuronal cells on catecholamine and acetylcholine synthesis and accumulation in cultures of associated sympathetic neurons. Proceedings of the National Academy of Sciences, 71, 3607-3610.
- Perlmutter, L.S., Tweedle, C.O., & Hatton, G.I. (1984). Neuronal/glial plasticity in the supraoptic dendritic zone: Dendritic bundling and double synapse formation at parturition. Neuroscience, 13, 769-779.
- Rosenzweig, M.R., & Bennett, E.L. (1972). Cerebral changes in rats exposed individually to an enriched environment. Journal of Comparative and Physiological Psychology, 80, 304-313.
- Sharp, P.E., McNaughton, B.L., & Barnes, C.A. (1985). Enhancement of hippocampal

- field potentials in rats reared in complex environments: Evidence from hippocampal slices maintained *in vitro*. Journal of Neurophysiology, **55**, 739-750.
- Sirevaag, A.M., & Græenough, W.T. (1987). Differential rearing effects on rat visual cortex synapses. III. Neuronal and glial nuclei, boutons, dendrites, and capillaries. Brain Research, **424**, 320-332.
- Skelton, R.W., Scarth, A.S., Wilke, D.M., Miller, J.J., & Phillips, A.G. (1987). Long-term increases in dentate granule cell responsivity accompany operant conditioning. Journal of Neuroscience, **7**, 3081-3087.
- Squire, L.R., & Butters, N. (Eds.). (1984). Neuropsychology of Memory. New York: Guilford Press.
- Szeligo, R., & Leblond, C.P. (1977). Response of the three main types of glial cells of cortex and corpus callosum in rats handled during suckling or exposed to enriched, control, and impoverished environments following weaning. Journal of Comparative Neurology, **172**, 247-264.
- Teyler, T.J., & DiScenna, P. (1987). Long-term potentiation. Annual Review of Neuroscience, **10**, 131-161. Palo Alto: Annual Reviews.
- Turner, A.M., & Greenough, W.T. (1985). Differential rearing effects on rat visual cortex synapses: I. Synaptic and neuronal density and synapses per neuron. Brain Research, **329**, 195-203.
- Tweedle, C.D., & Hatton, G.I. (1976). Ultrastructural comparisons of neurons of supraoptic and circularis nuclei in normal and dehydrated rats. Brain Research Bulletin, **1**, 103-121.
- Virchow, R. (1859). Cellularpathologie. Trans. F. Chance. Hirschwald: Berlin.
- Weibel, E.R. (1979). Stereological Methods, **1**. Practical Methods for Biological Morphometry. New York: Academic.
- Weisz, D.J., Clark, G.A., Thompson, R.F., & Solomon, P.R. (1982). Activity of dentate

gyrus during NM conditioning in rabbit. In Conditioning, vol. 26. New York: Plenum Press.

Wolff, J.R., & Guldner, F.-H. (1978). Perisynaptic astroglial reactions to neuronal activity. In E. Schoffeniels, G. Franck, L. Hertz, & D.B. Tower (Eds.), Dynamic Properties of Glia Cells (pp. 115-118). New York: Pergamon Press.

Young, J.A.C., Brown, D.A., Kelly, J.S., & Schon, F. (1973). Autoradiographic localization of sites of [3H]-aminobutyric acid accumulation in peripheral autonomic ganglia. Brain Research, 63, 479-486.

Author Notes

The completion of this thesis would not have been possible without the assistance of many people. First of all, I would like to thank Dr. William T. Greenough for all his guidance and support over the last two years, and for allowing me to participate in his research as an undergraduate. I would next like to thank Krystyna Isaacs and Anita Sirevaag for helping me through every stage of the process of completing this thesis. I would also like to gratefully acknowledge the contributions of Drs. F.-L. Chang and Robert Henderson in providing me invaluable advice and information .

Figure Captions

Figure 1. A hippocampal field potential representing a population of synchronously active neurons. A line is drawn from point A to C and the area below this line is the spike area. The average of the length of line AB and BC is the spike height. The spike area and the spike height are used to confirm the presence of LTP.

Figure 2. A schematic diagram of the trisynaptic circuit; the three synapses are (1) entorhinal axons to dentate granule cells via the perforant path (pp); (2) granule cells to CA3 pyramidal cells via the mossy fiber pathway (mf) and (3) CA3 pyramidal cells to CA1 pyramidal cells via Schaeffer collaterals (Sch).

Figure 3. Long-term potentiation of the population response. (A) Pre-LTP (B) Post-LTP. Note decreased latency (time between artifact and spike) of population spike, larger spike, and steeper EPSP slope in the post-LTP response.

Figure 4. Spine, shaft, and sessile synapses on a dendrite.

Figure 5. A fibrous astrocyte potentially provides a route for nutritive transfer among capillaries, glia, and neurons.

Figure 6. Indirect immunocytochemical staining for glial fibrillary acidic protein (GFAP). This technique involves a layering of first a primary antibody that uses GFAP as the antigen, and next a secondary antibody that uses the primary antibody as the antigen. An avidin-biotin complex labelled with peroxidase is then added, and finally diaminobenzidine (DAB) is added to develop the peroxidase and visualize the reaction.

Figure 7. The cycloid grid. Used to provide a stereologically unbiased estimate of the surface area of glial cell processes.

Figure 8. Astrocytic surface density (S_v) in inverse microns. S_v is highest in the outer third of the molecular layer and progressively decreases as one approaches the granule cell layer.

Figure 9. Astrocytic Sv in stratum radiatum of hippocampal CA1 region. There is no statistical difference between thirds in this region.

Figure 10. Astrocytic process thickness in the dentate gyrus molecular layer decreases, on the average, as one moves from the outer third of the molecular layer to the innermost third. Thickness categories are 1,2,3,4, and 5, where 1—a process thickness less than 1 μm , and 5—a process thickness greater than 3.5 μm . The values of 2,3, and 4 lie between these values.

Figure 11. At 100 μm from the recording electrode tip there were no significant differences in Sv between the LTP and the AC groups when analyzed across all thirds of the molecular layer.

Figure 12. At 100 μm from the recording electrode tip there was a significant increase in the absolute frequency of processes of thickness 1 in the LTP group in the middle third of the molecular layer. In the outer third there was a significant increase in processes of thickness 2 in the LTP group.

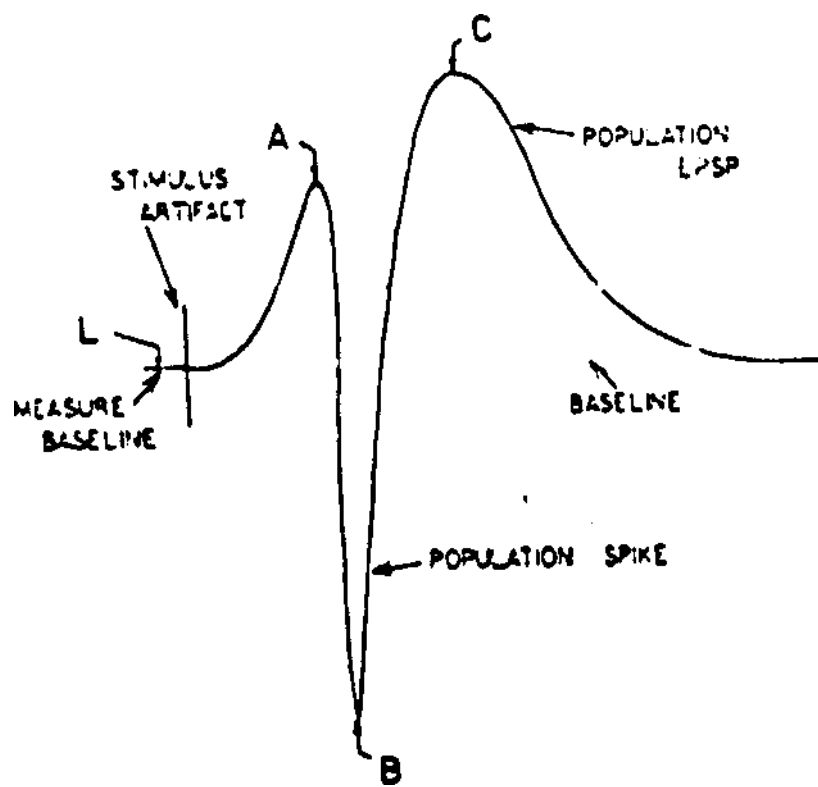
Figure 13. When measured at 200 μm from the recording electrode tip, Sv was greater in all thirds of the molecular layer for the LTP group, but this difference failed to reach acceptable levels of significance.

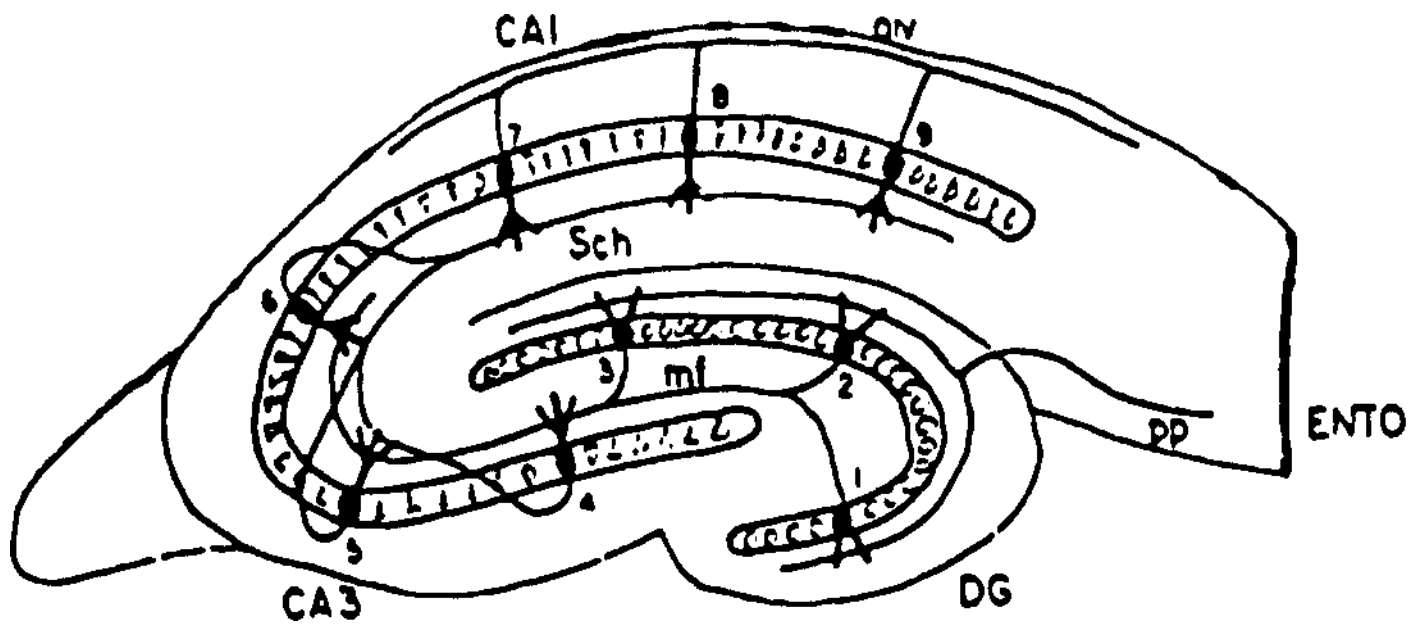
Figure 14. At 200 μm from the recording electrode tip, the absolute frequency of processes of thickness 3 was significantly greater in the LTP group for all thirds of the molecular layer. In the outer third, the frequency of processes of thicknesses 4 and 5 was significantly greater in the LTP group.

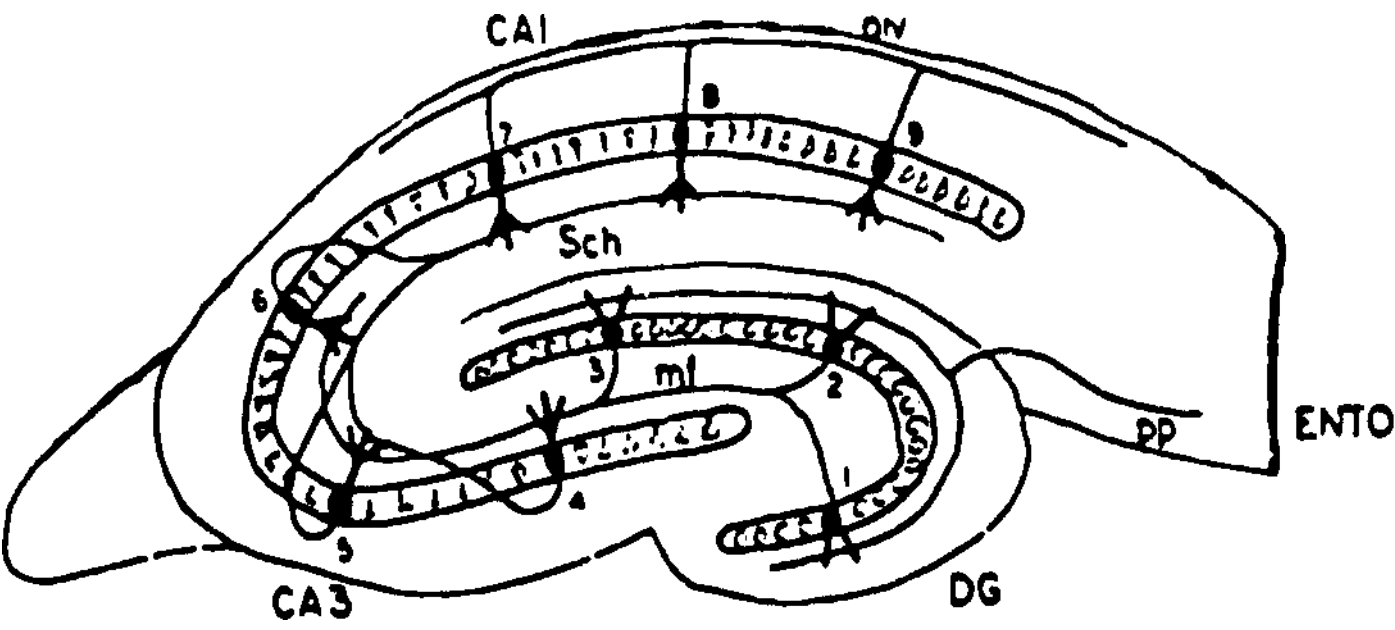
Figure 15. At 300 μm from the recording electrode tip, when analyzed across all thirds there were no statistically significant differences in Sv between the LTP and the AC groups.

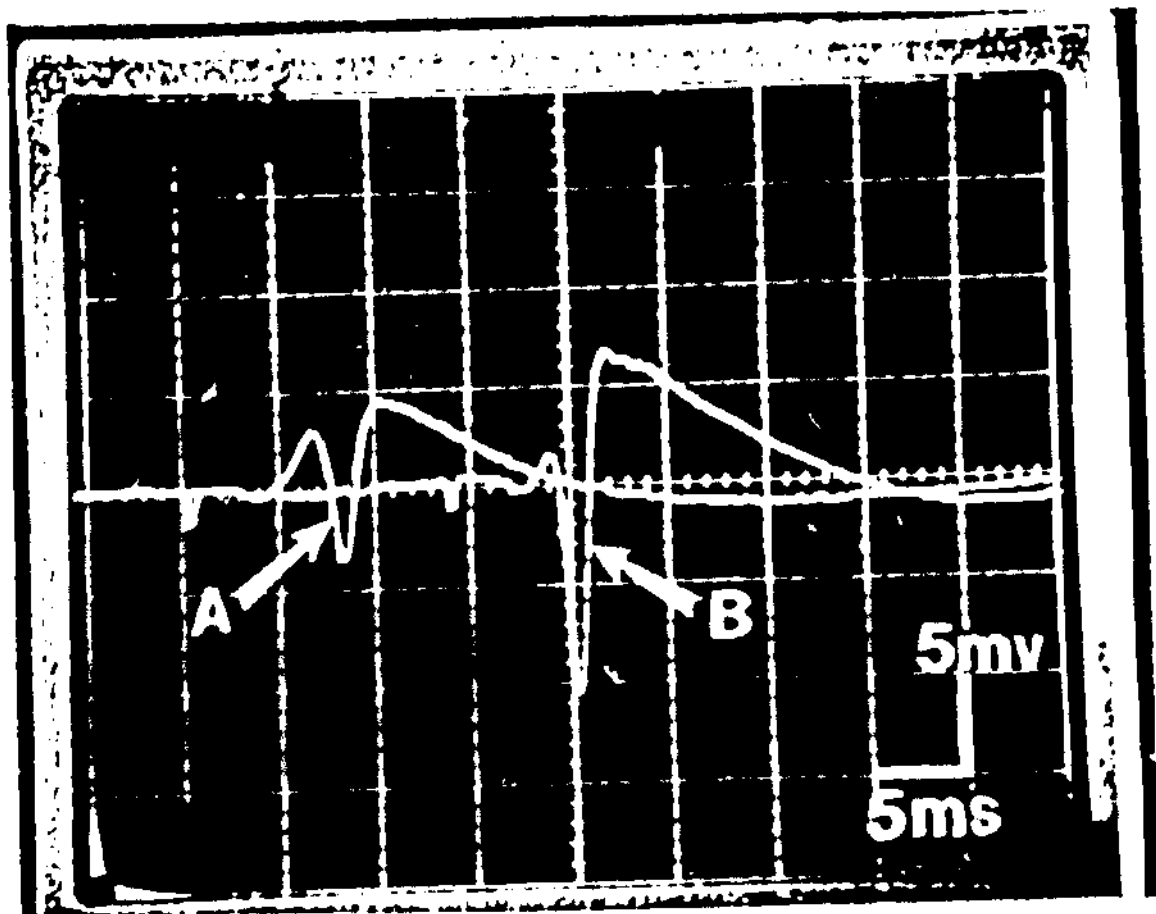
Figure 16. At 400 μ m from the recording electrode tip, the astrocytic Sv was significantly greater for the LTP condition than the AC condition when analyzed across all thirds of the molecular layer.

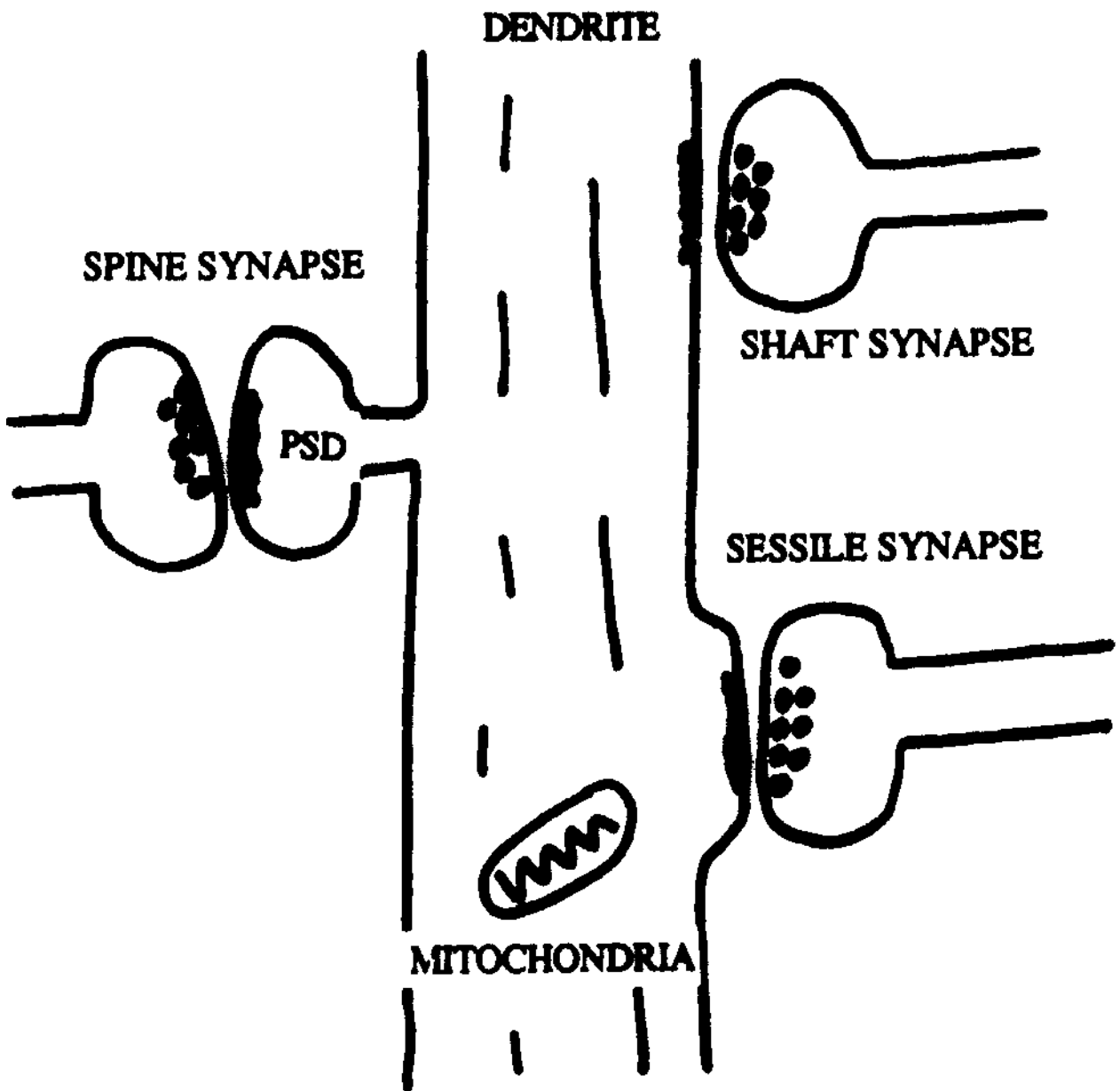
Figure 17. At 400 μ m from the electrode tip, in all thirds of the molecular layer there were increased absolute frequencies of processes of thickness 4 and 5 for the LTP group. In the middle and inner thirds of the molecular layer there were increased absolute frequencies of processes of thickness 3 for the LTP group. There were no significant differences in the absolute frequencies of processes of thicknesses 1 and 2 combined between the LTP and AC groups.

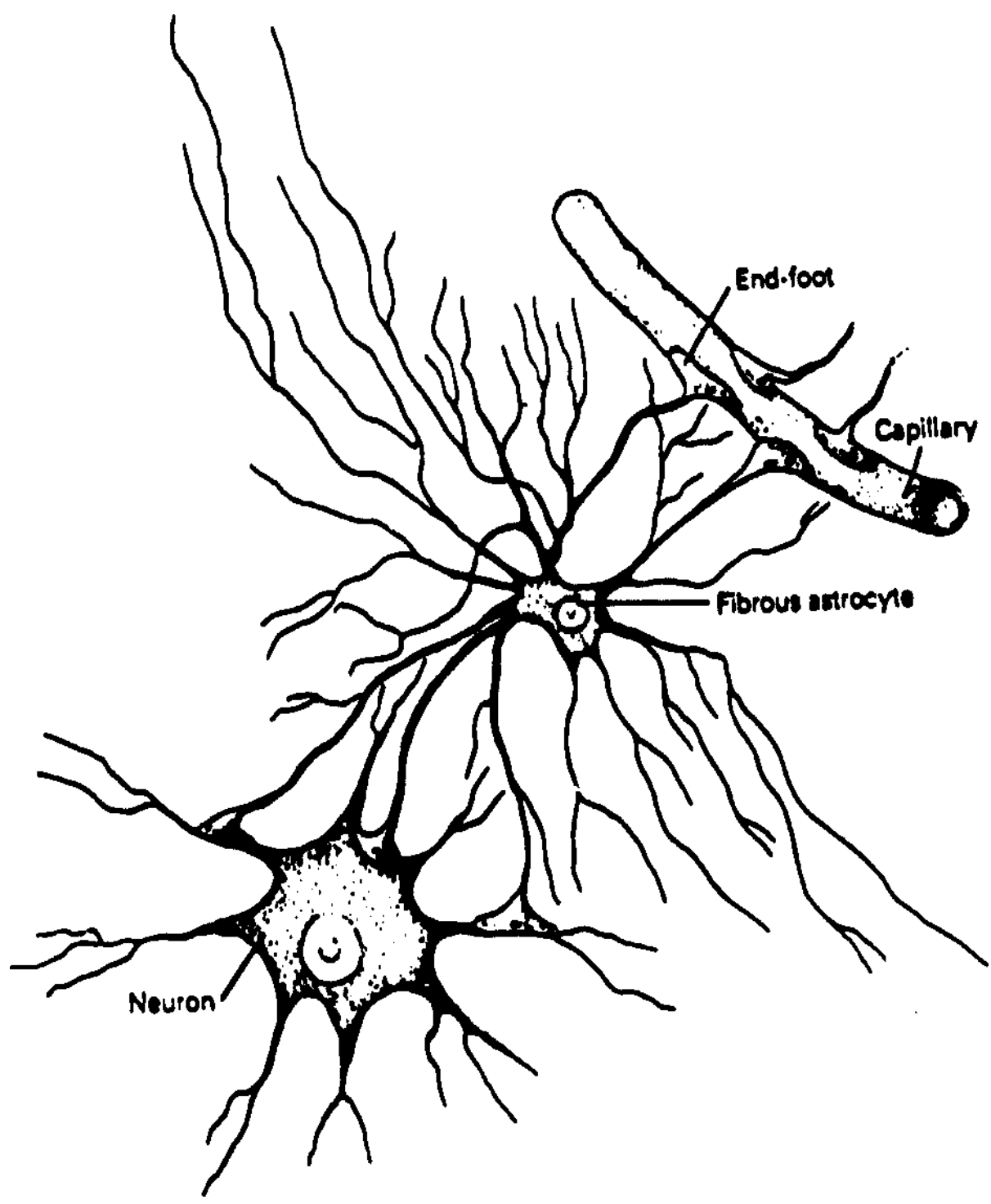


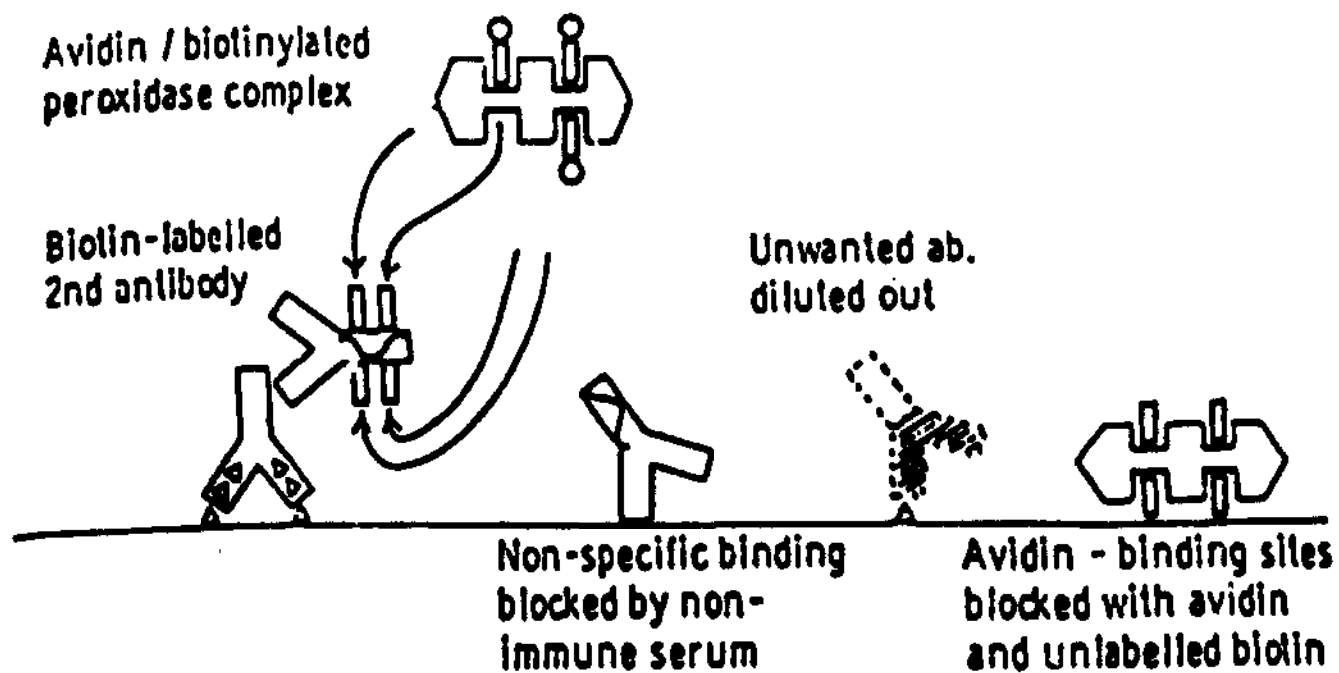


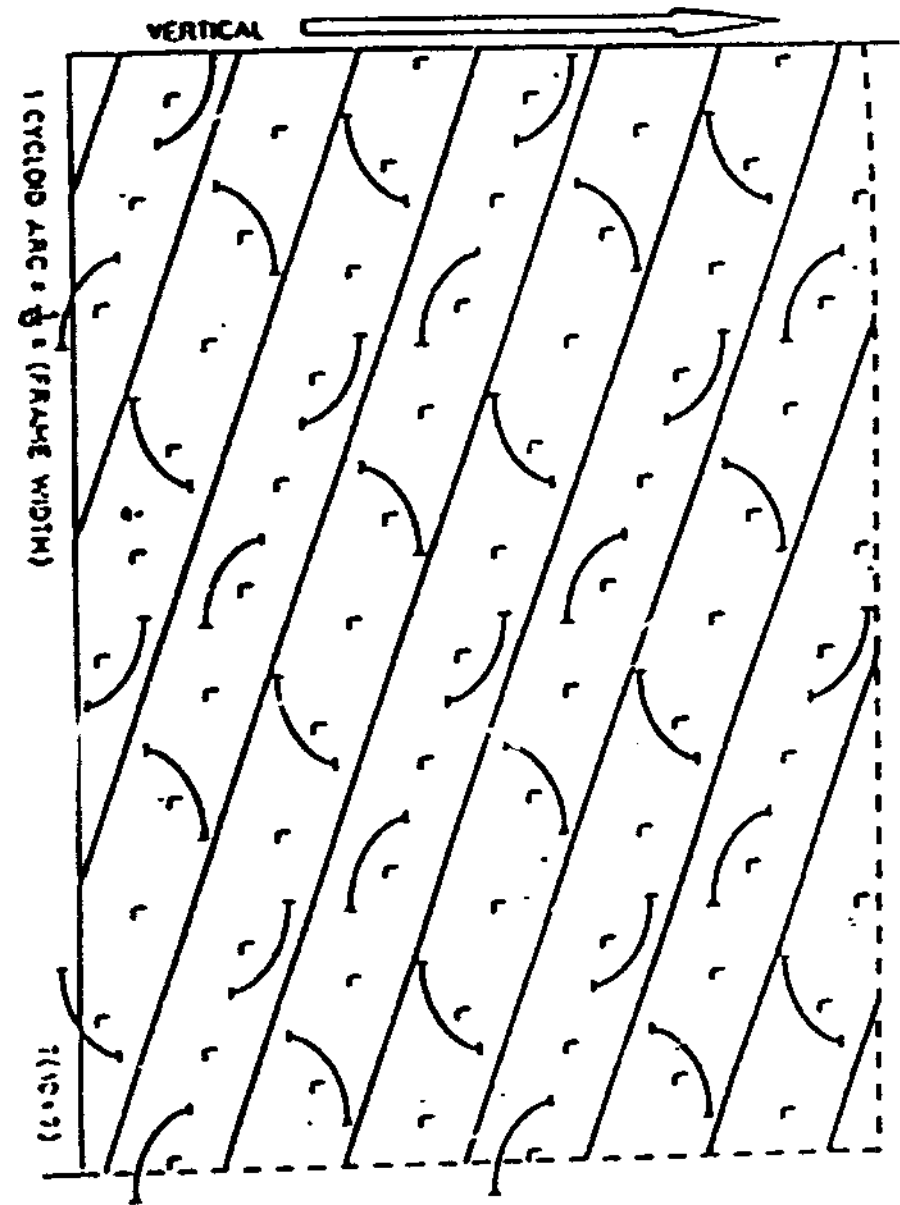




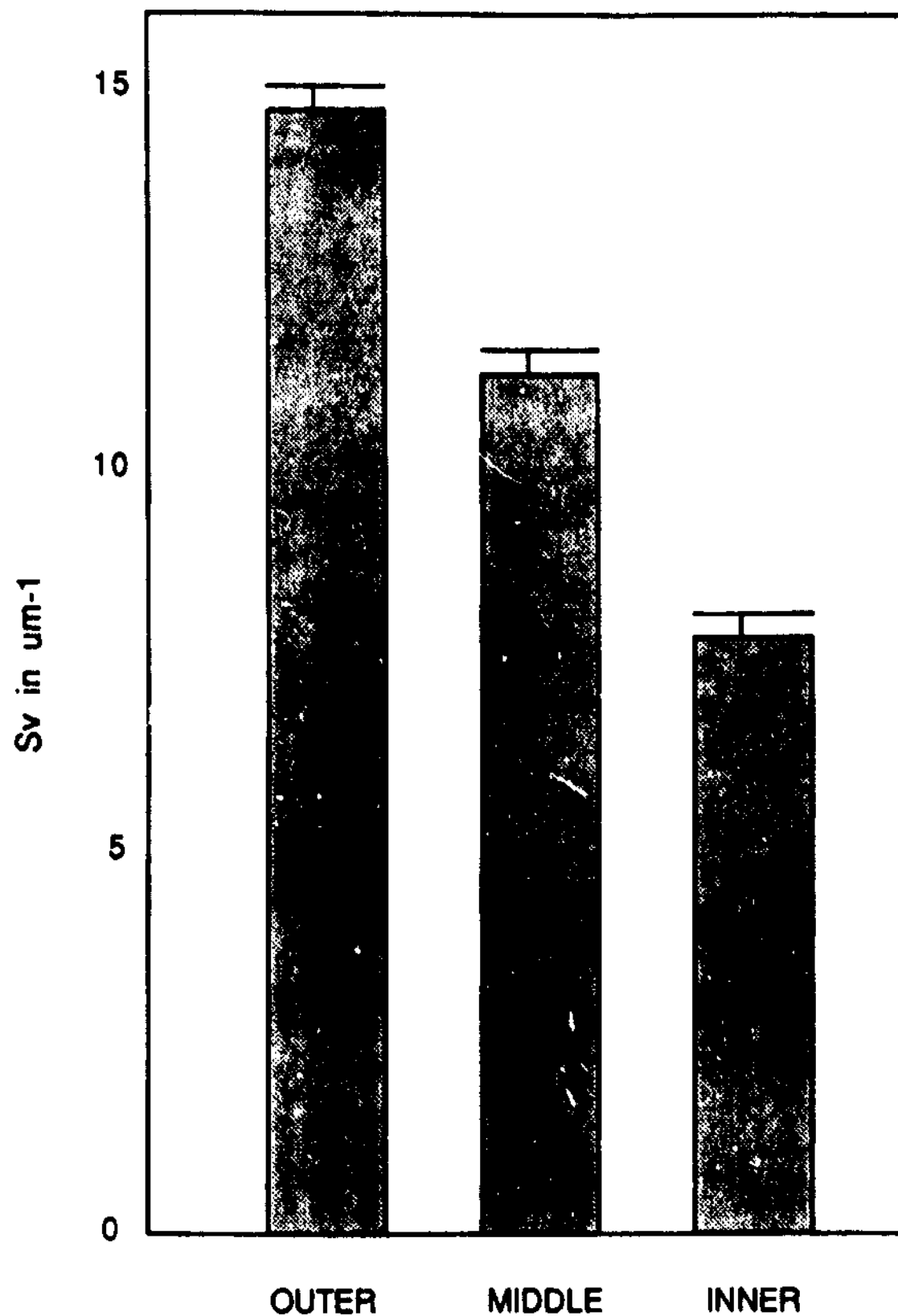






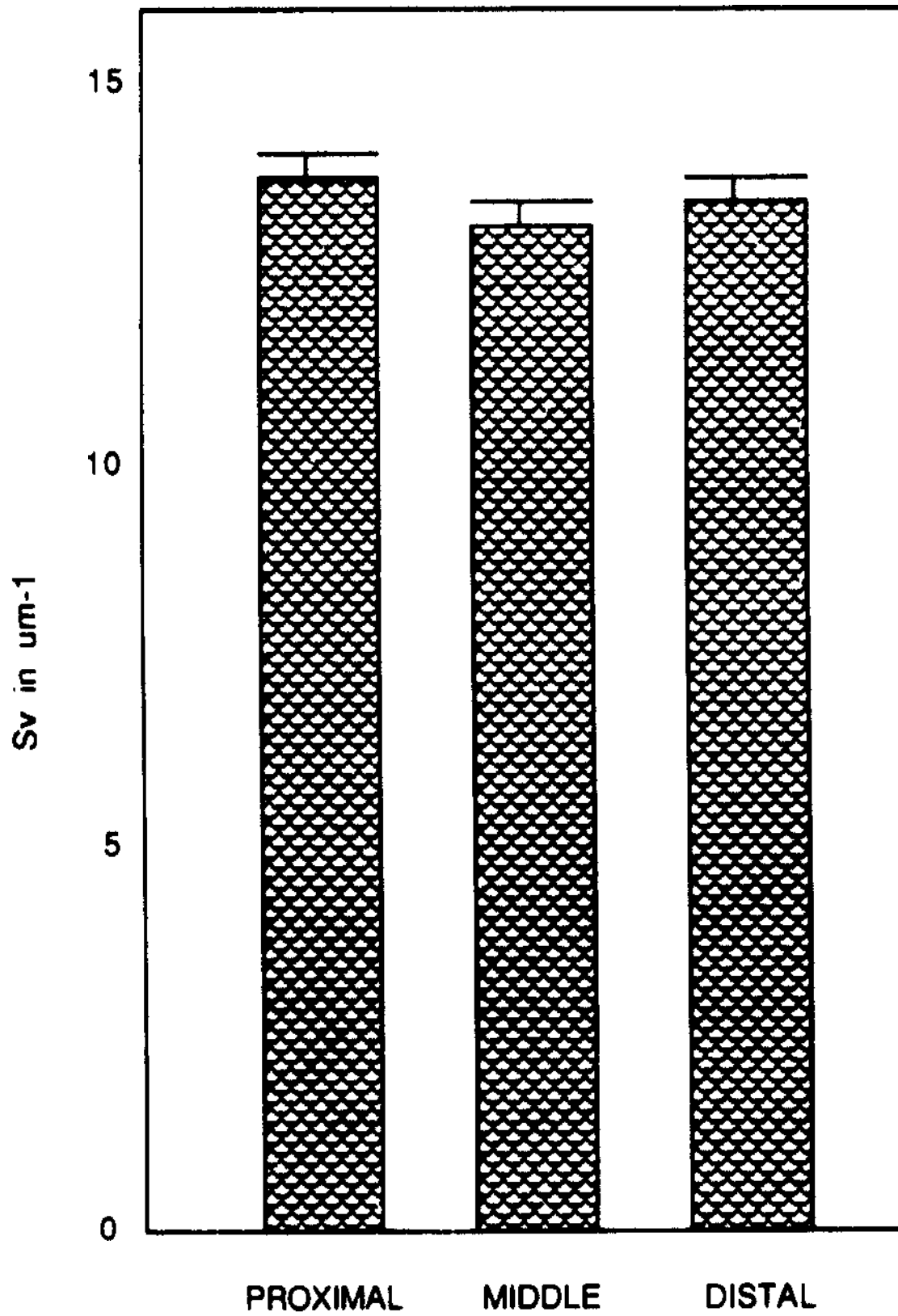


ASTROCYTIC SURFACE DENSITY IN DENTATE MOLECULAR LAYER



ANOVA: $F=165.79$ $p<0.0001$; STUDENT NEWMAN-KEULS: $p<0.01$
SURFACE DENSITY IN ALL THIRDS ARE DIFFERENT FROM EACH OTHER

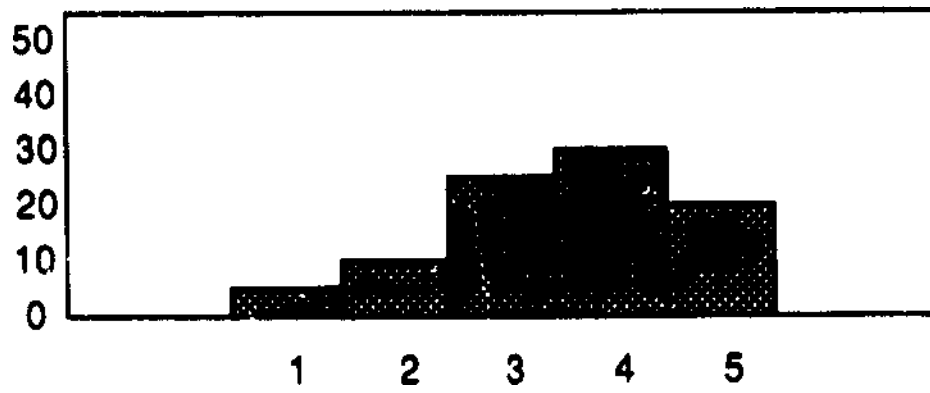
ASTROCYTIC SURFACE DENSITY IN S. RADIATUM OF CA1



THE THREE SAMPLES ARE NOT STATISTICALLY DIFFERENT
 $F=0.19, p>0.05$

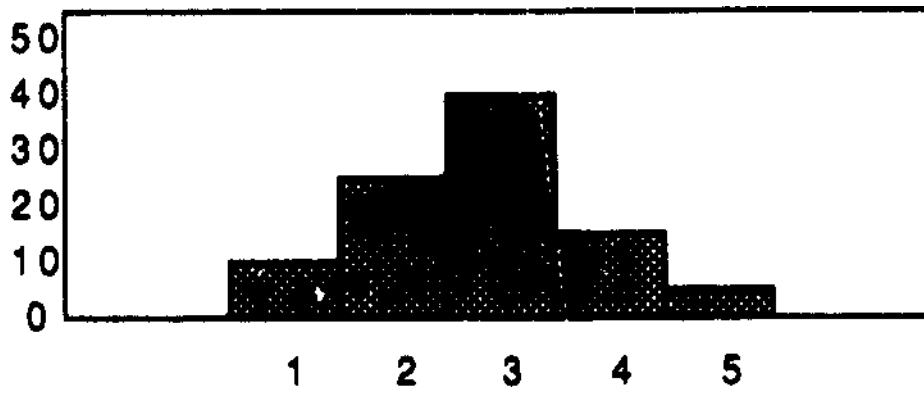
ASTROCYTIC PROCESS THICKNESS IN DENTATE MOLECULAR LAYER

OUTER THIRD

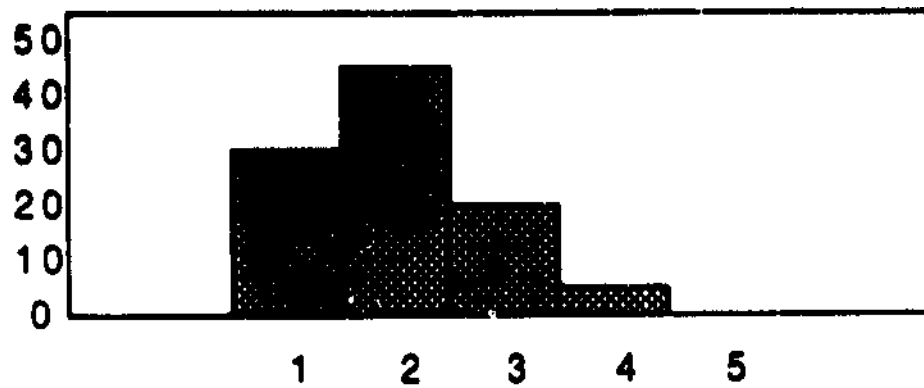


MIDDLE THIRD

RELATIVE FREQUENCY

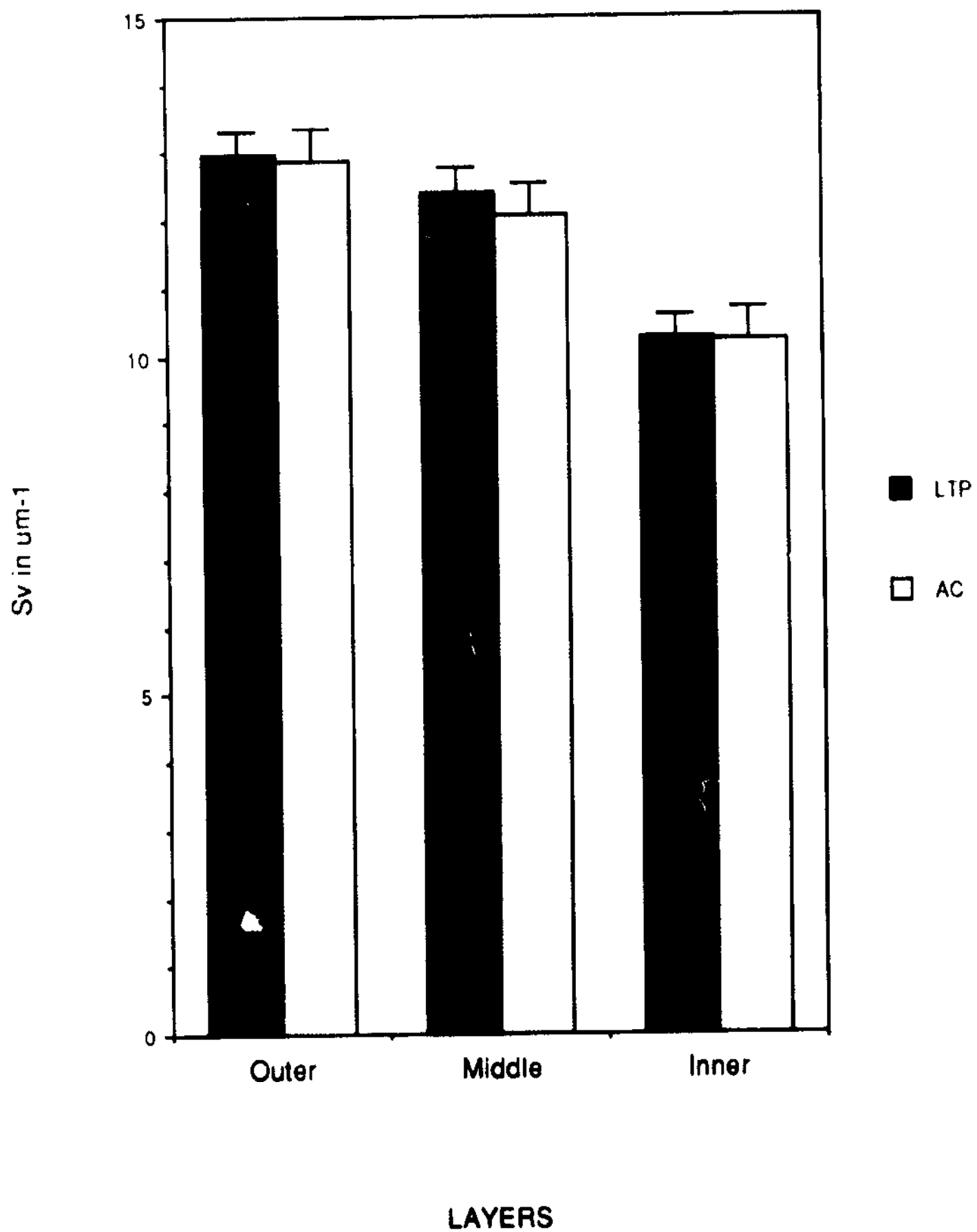


INNER THIRD

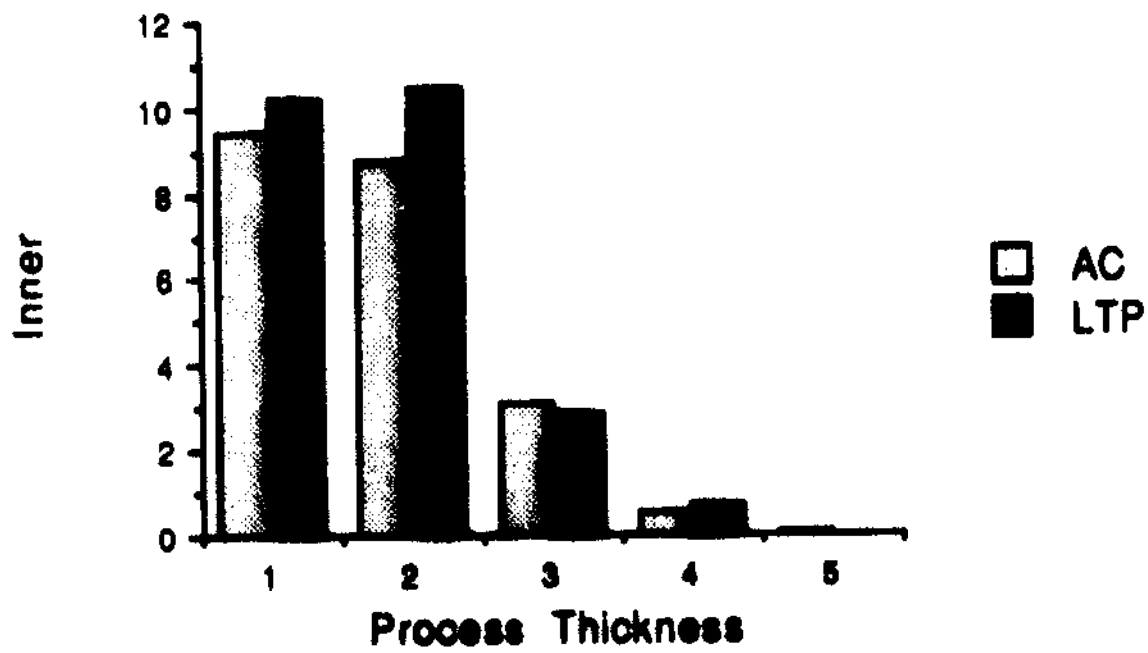
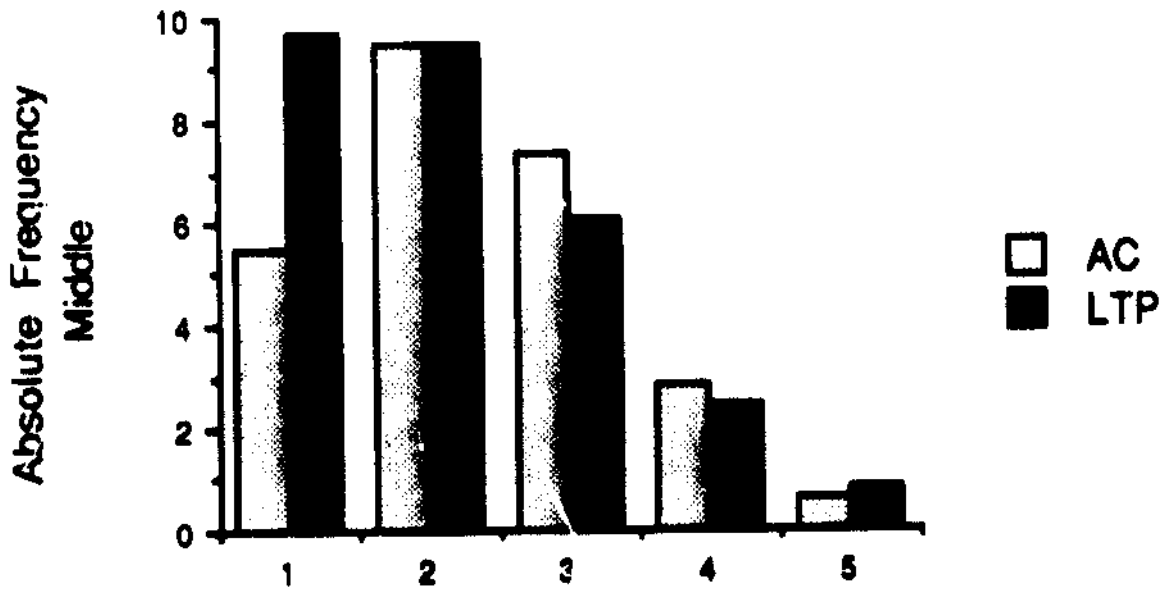
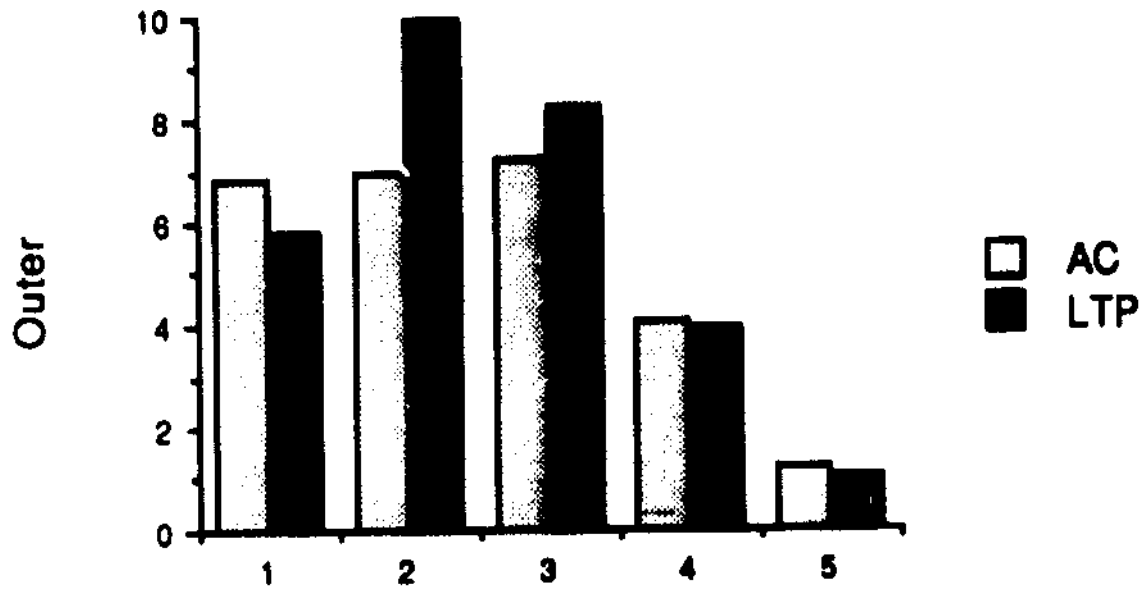


THICKNESS CATEGORIES

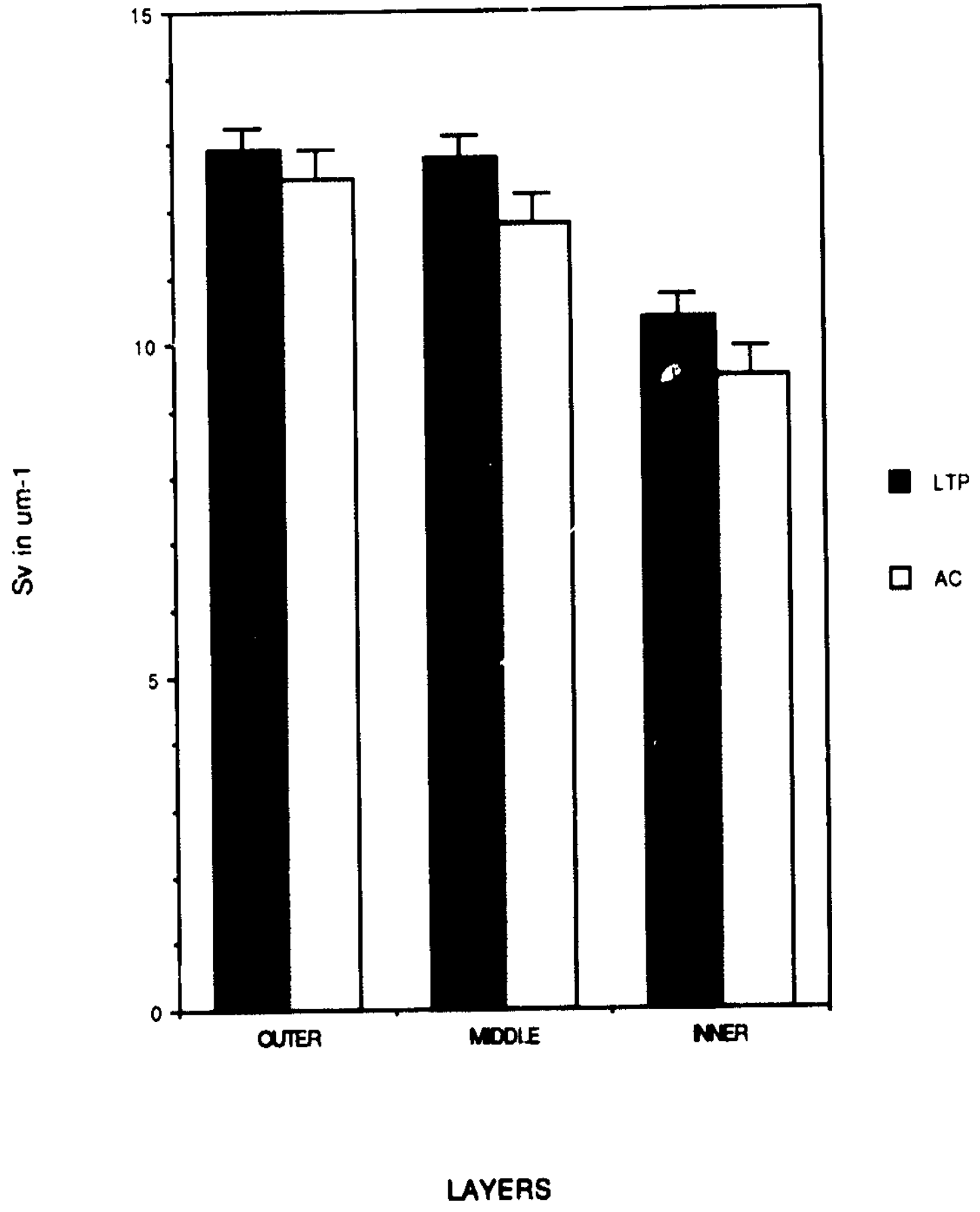
ASTROCYTIC Sv AT 100 μm FROM ELECTRODE TIP



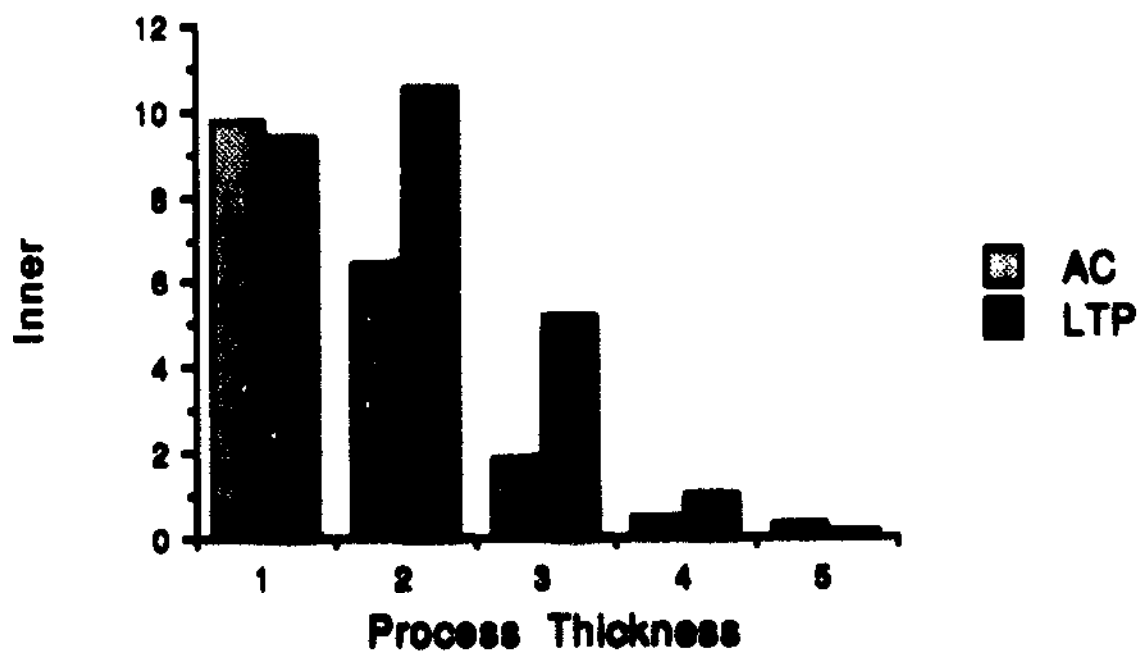
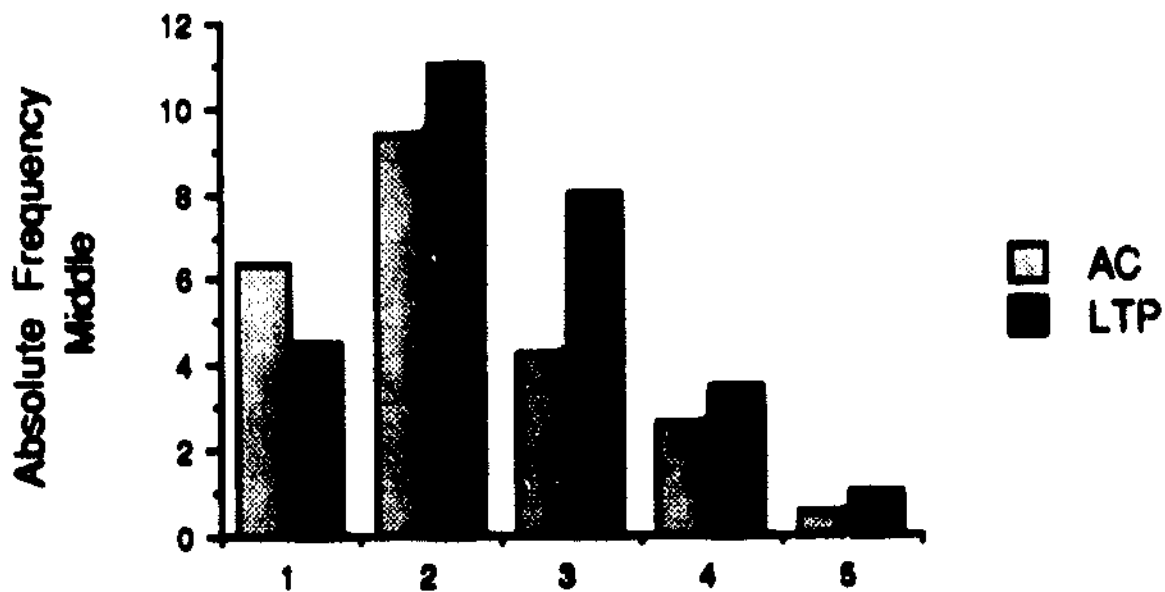
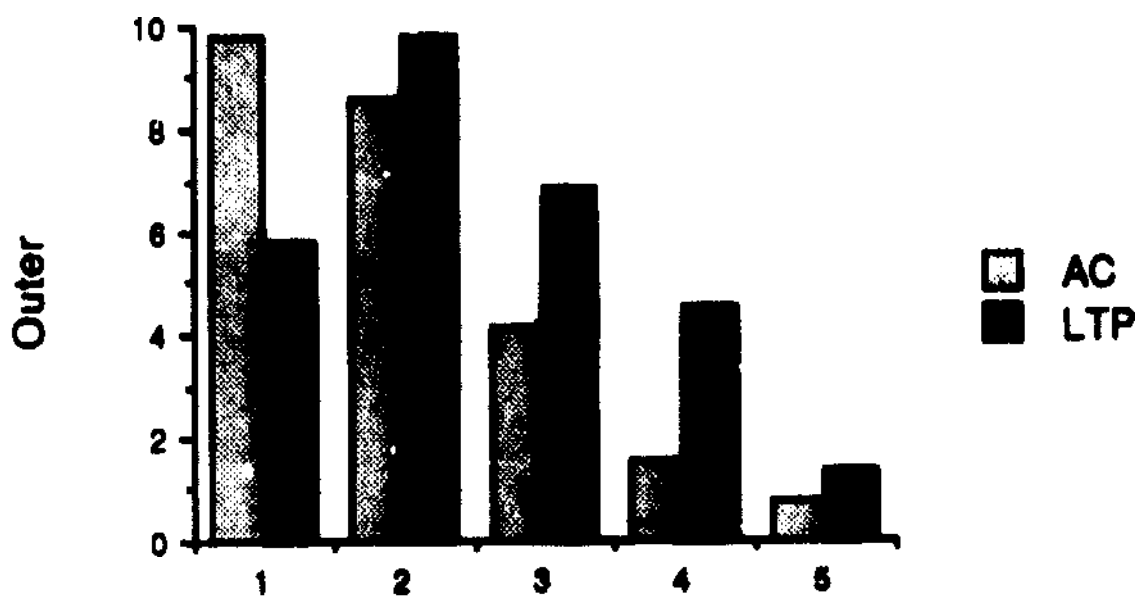
Process Thickness at 100 um



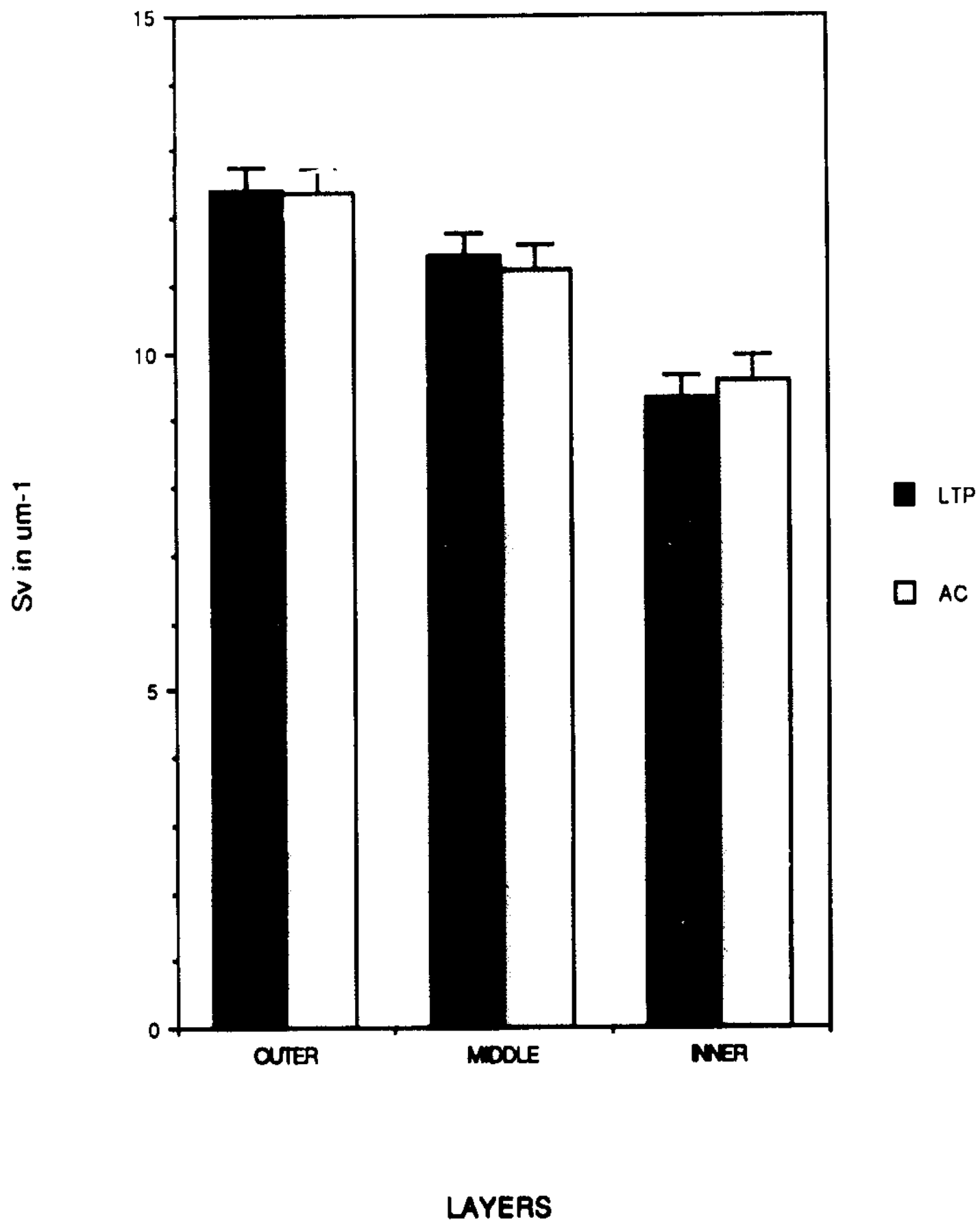
ASTROCYTIC Sv AT 200 μm FROM ELECTRODE TIP



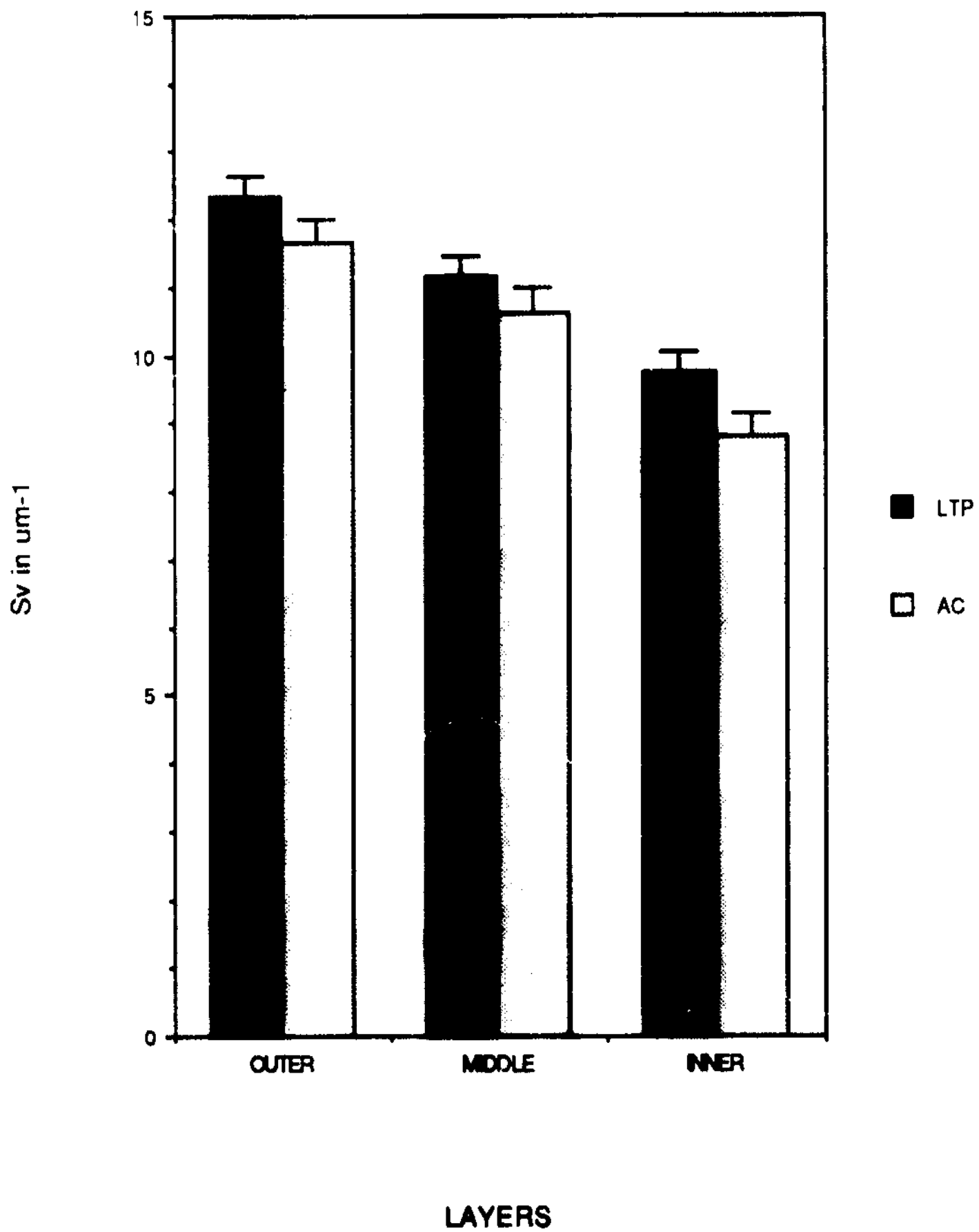
Process Thickness at 200 um



ASTROCYTIC Sv AT 300 μm FROM ELECTRODE TIP



ASTROCYTIC Sv AT 400 μm FROM ELECTRODE TIP



Process Thickness at 400 um

